To appear in the *International Journal of Control*
Vol. 00, No. 00, Month 20XX, 1–28

This is a pre-print of an article published by Taylor & Francis in
International Journal of Control on 2018-02-27, available online:
https://doi.org/10.1080/00207179.2018.1438668

A modified sliding mode observer design with application to diffusion

S. Afshar[a*], K. A. Morris[a], and A. Khajepour [b]

[a]*Department of Applied Mathematics, University of Waterloo, Canada;* [b]*Department of Mechanical and Mechatronics Engineering, University of Waterloo, Canada*

(*Received 00 Month 20XX; accepted 00 Month 20XX*)

In many physical systems, the system's full state cannot be measured. An observer is designed to reconstruct the state from measurements. Disturbances often contribute to the dynamics of the system, and the designed observer must account for them. In this paper, a modified sliding model observer (SMO), a robust observer, is proposed that combines the efficiency of a nonlinear observer with the robustness of a SMO. The estimation error is proven to converge to zero under natural assumptions. This improved observer is compared with an extended Kalman filter and an unscented Kalman filter, as well as a standard SMO for three different versions of heat equation: a linear, a quasi-linear, and a nonlinear heat equation. The comparisons are done with and without an external disturbance. The simulations show improved performance of the modified SMO over other observers.

Keywords: Robust observer; Distributed parameter systems; Heat equation; Observer design; Sliding mode observer; Kalman filtering.

1. Introduction

In many physical systems, the full state of the system is important; however, it cannot be measured. Observer design is a well-known approach for reconstructing the state vector from some measured quantities. The observer dynamics are composed of a copy of the system's dynamics and a feedback term.

Although the observer design for the systems represented by linear ordinary differential equations (ODEs) is well studied (see Misawa and Hedrick (1989) for a review), it can be challenging for nonlinear systems. A comparison of nonlinear observers for ODEs can be found in Walcott, Corless, and Żak (1987) and Chen and Dunnigan (2002). Some nonlinear systems can be transformed into a linear form for which the observer can be adjusted as in Kazantzis and Kravaris (1998), Xia and Gao (1989), Noh, Jo, and Seo (2004), Ding, Frank, and Guo (1990), Rigatos (2011), Rigatos (2015a), and Rigatos (2015b). Checking the necessary and sufficient conditions for the existence of such a transformation is not easy; this transformation might not exist in a general case. Among different nonlinear observers, extended Kalman filter (EKF) and unscented Kalman filter (UKF) are two nonlinear efficient yet simple estimation techniques (see Grewal and Andrews (2011) and Wan and Van Der Merwe (2000) for details).

The existence of disturbances in most physical models is inevitable and adds more complications to the observer design. A robust observer is intended to compensate for the disturbances; examples can be found in Kai, Wei, and Liu (2010), Kai, Liangdong, and Yiwu (2011), Einicke and White (1999), and Reif, Sonnemann, and Unbehauen (1999). These observers are efficient in

*Corresponding author. Email: safshar@uwaterloo.ca

compensating for multiplicative disturbances and zero mean bounded noises. A different approach is implementing sliding mode techniques in which the disturbances are modeled by some unknown inputs. In this case, no restriction except for boundedness is made on the disturbances. Sliding mode techniques were first employed for observation in the 1980's (see Walcott and Zak (1987)) and were incorporated in the design of a robust observer called a sliding mode observer (SMO). A good review of sliding mode observation methods for both linear and nonlinear systems can be found in Spurgeon (2008). The idea is to use a discontinuous output feedback to drive the estimation state vector towards a reference manifold. The main advantages of the SMO are insensitivity to unknown inputs, robustness, and providing an equivalent output error injection that can also be used as a source of information Fridman, Shtessel, Edwards, and Yan (2008). An important challenge is how the disturbances can be included in the observer design. In general, the consideration of the disturbances induces either structural conditions or matching assumptions to ensure a finite time convergence towards the sliding surface Veluvolu, Soh, and Cao (2007a). Different designs handle the disturbances and system nonlinearities in different ways; see Drakunov and Utkin (1995), Utkin (1999), Xiong and Saif (2001), Drakunov (1992), Drakunov and Reyhanoglu (2011), Xiong and Saif (2001), and Koshkouei and Zinober (2004).

As a robust estimation technique, a Luenberger observer is usually used with the SMO; for instance, see Spurgeon (2008), Koshkouei and Zinober (2004), and Veluvolu, Soh, and Cao (2007b). For a nonlinear system, the Luenberger observer must overcome the nonlinearities and stabilize the error dynamics on the sliding surface. Generally, a linear matrix inequality (LMI) problem is solved to obtain the Luenberger observer as in Koshkouei and Zinober (2004) and Veluvolu et al. (2007b). The LMI problem is not easy to solve; in fact, it might have no solution.

In this paper, a modified version of the SMO is developed. Instead of the Luenberger observer, the modified SMO combines an exponentially stabilizing nonlinear observer with the sliding mode observation to increase the estimation performance. The exponential convergence of the estimation error to zero is proven. The improved observer can compensate for both nonlinearities and disturbances coming from an unknown input.

In some physical processes, such as diffusion, the system's behavior is distributed in space. These systems are known as distributed parameter systems (DPSs) and are modeled by partial differential equations. Observer design for linear DPSs has been well studied; for instance, see Sallberg, Maybeck, and Oxley (2010), Smyshlyaev and Krstic (2005), Hidayat, Babuska, De Schutter, and Nunez (2011), Liu and Lapldus (1976), Miranda, Chairez, and Moreno (2010), Orlov (2008), Curtain (1982), Demetriou (2004), Meirovitch and Baruh (1983), and also the book Curtain and Zwart (1995). However, observer design has not been well explored for nonlinear DPSs. Some examples of observer design for the nonlinear DPSs can be found in Wu and Li (2008), Wu and Li (2011), and Castillo, Witrant, Prieur, and Dugard (2013).

A major issue in the observer design for DPSs is that the original partial differential equations cannot in general be used in the observer dynamics. The usual way of dealing with this problem is to approximate the system by a system of ODEs via some approximation method, such as the finite element method. This approximation introduces errors into the observer's dynamics because the higher modes are neglected. In this paper, this truncation is treated as a disturbance to an ODE model. It is proven that for a wide class of nonlinear PDEs, the modified SMO provides estimation with an error that goes to zero as the order of approximation of the observer is increased.

The performance of the modified SMO is compared with two well-known nonlinear observers, the EKF and UKF and a standard SMO for three different versions of the diffusion equation: a linear, a quasi-linear, and a nonlinear model. Two sources of uncertainties are introduced in the observer design: the disturbances coming from the unknown input $\xi(t)$ and the modeling uncertainty due to the order reduction in the observer design. The simulation results show that the modified SMO performs better than the other observers in the presence of external disturbances and model truncation.

2. Observer design

Consider the following ordinary differential equation model consisting of n differential equations:

$$\begin{aligned} \frac{d\mathbf{z}_{orig}(t)}{dt} &= \boldsymbol{f}(\mathbf{z}_{orig}(t)) + \boldsymbol{B}u(t) + \boldsymbol{g}(\mathbf{z}_{orig}(t))\xi(t), \qquad \mathbf{z}_{orig}(0) = \boldsymbol{z}_{orig,0}, \\ y(t) &= \boldsymbol{C}\mathbf{z}_{orig}(t) \end{aligned} \tag{1}$$

where $\mathbf{z}_{orig}(t) \in \mathbb{R}^n$ is the state variable, $u(t) \in \mathbb{R}$ is the control, $\xi(t) \in \mathbb{R}$ is the disturbance input and $y(t) \in \mathbb{R}$ is the measured output. Here $\boldsymbol{B} \in \mathbb{R}^{n\times 1}$, $\boldsymbol{C} \in \mathbb{R}^{1\times n}$, $\boldsymbol{f}(\cdot)$ and $\boldsymbol{g}(\cdot)$ are smooth vector fields on $\mathbb{R}^n$. The vector field $\boldsymbol{g}(\cdot)$ is called the distribution vector and indicates the disturbance spatial distribution. The disturbance input is assumed to be bounded, that is a positive number M_ξ exists such that $|\xi| \leq M_\xi$.

For simplicity of exposition, consider a discrete-time implementation

$$\begin{aligned} \boldsymbol{z}_{k+1} &= \boldsymbol{f}_d(\boldsymbol{z}_k) + \boldsymbol{B}_d u_k + \boldsymbol{\nu}_k \\ y_k &= h(\boldsymbol{z}_k) + \omega_k \end{aligned} \tag{2}$$

where $\boldsymbol{z}_k$, u_k, and y_k are, respectively, the state vector, input variable, and output at time step $t = t_k$, $\boldsymbol{\nu}_k$ is the system noise, and ω_k is the measurement noise.

The EKF algorithm is summarized in Table 1 where $\boldsymbol{z}_0$ is the state vector at time $t = t_0$, $\bar{\boldsymbol{s}} = E(\boldsymbol{s})$ represents the mean value of the random vector $\boldsymbol{s}$, and $a > 0$ defines the rate of exponential convergence. More details on this estimation technique can be found in Grewal and Andrews (2011). The exponential convergence, provided that certain assumptions are satisfied, of the EKF is shown to hold in Reif and Unbehauen (1999) and Reif, Sonnemann, and Unbehauen (1998).

(Table 1 near here)

The UKF is another candidate often used for nonlinear systems to provide an accurate estimation. In this technique, the variance is updated at each step via some sample points. For a random vector of dimension N, $2N+1$ sample points, which are also called sigma points, are used. Details can be found in Wan and Van Der Merwe (2000). The sigma points and their corresponding weights are

$$\begin{aligned} \boldsymbol{z}_{s,0} &= \bar{\boldsymbol{z}} \\ \boldsymbol{z}_{s,i} &= \bar{\boldsymbol{z}} \pm (\sqrt{(N+\lambda)\boldsymbol{P}_{\boldsymbol{z}}})_i \quad i = 1, \cdots, N \\ W_0^m &= \frac{\lambda}{N+\lambda}, \quad W_0^c = \frac{\lambda}{N+\lambda} + (1 - \alpha_0^2 + \beta) \\ W_i^m &= W_i^c = \frac{1}{2(N+\lambda)} \end{aligned} \tag{3}$$

where $\boldsymbol{z}_{s,i}$ for $i = 0, \cdots, 2N$ are sample points, W_i^m for $i = 0, \cdots, 2N$ are associated weights for calculation of the means, W_i^c for $i = 0, \cdots, 2N$ are associated weights for the covariance calculation, $\lambda = \alpha_0^2(N+\kappa) - N$ is a scaling parameter, and α_0, κ are tuning parameters. The algorithm is given in Table A.

(Table A near here)

Unmodelled disturbances are often present. A robust observer is required to compensate for the disturbances. A potential way of including robustness in the observer design is to employ sliding mode techniques in which no assumption except for boundedness is made on the unknown input to compensate for its presence.

The first step in the SMO design is to transform the system representation (1) into a standard form as in Xiong and Saif (2001). The transformation divides the system into two parts: the part which is directly affected by the unknown input and the part which is not.

The following assumptions on the system are required.

Assumption 1: *The functions* $\boldsymbol{f}(\cdot)$ *and* $\boldsymbol{g}(\cdot)$ *are smooth vector fields up to the* n*th order. In other words, they are continuously differentiable of the* n*th order with respect to their arguments.*

Assumption 2: *Let a standard definition of relative degree for the system (1) be used as in Isidori (1995). The relative degree of the system (1) from the input* $\xi(t)$ *to the output* $y(t)$ *is independent of* $\boldsymbol{z}_p \in \mathcal{R}^n$*.*

If $\boldsymbol{C}\boldsymbol{g}(\boldsymbol{z}_p(t)) \neq 0$ for every $\boldsymbol{z}_p(t) \in \mathcal{R}^n$ the system has the relative degree one and satisfies Assumption 2. This is not a hard condition to check and often holds in the observer design.

Let the relative degree be q. If Assumption 2 holds, $q \leq n$ (Isidori, 1995, Prop. 5.1.2). Set

$$\begin{aligned}
\phi_1(\mathbf{z}_{orig}(t)) &= \boldsymbol{C}\mathbf{z}_{orig}(t)\\
\phi_2(\mathbf{z}_{orig}(t)) &= L_{\boldsymbol{f}}\boldsymbol{C}\mathbf{z}_{orig}(t)\\
&\vdots\\
\phi_q(\mathbf{z}_{orig}(t)) &= L_{\boldsymbol{f}}^{q-1}\boldsymbol{C}\mathbf{z}_{orig}(t).
\end{aligned}$$

If $q < n$, $n-q$ functions, $\phi_{q+1}(\mathbf{z}_{orig}(t)), \cdots, \phi_n(\mathbf{z}_{orig}(t))$, can be found such that the Jacobian matrix of the mapping

$$\boldsymbol{z}_c(t) = \boldsymbol{\phi}(\mathbf{z}_{\boldsymbol{orig}}(\boldsymbol{t})) = \mathrm{col}(\phi_1(\mathbf{z}_{orig}(t)), \cdots, \phi_q(\mathbf{z}_{orig}(t)), \phi_{q+1}(\mathbf{z}_{orig}(t)), \cdots, \phi_n(\mathbf{z}_{orig}(t))) \tag{4}$$

is nonsingular at every $\boldsymbol{z}_p(t) \in \mathcal{R}^n$. Define the new state vector $\boldsymbol{z}_c^T(t) = [\boldsymbol{z}_d^T(t), \boldsymbol{z}_r^T(t)]$ where

$$\begin{aligned}
\boldsymbol{z}_d(t) &= \mathrm{col}(\phi_1(\mathbf{z}_{orig}(t)), \cdots, \phi_q(\mathbf{z}_{orig}(t)))\\
\boldsymbol{z}_r(t) &= \mathrm{col}(\phi_{q+1}(\mathbf{z}_{orig}(t)), \cdots, \phi_n(\mathbf{z}_{orig}(t))).
\end{aligned}$$

Define functions $a_d(\cdot)$, $c(\cdot)$, and $b_k(\cdot)$ produced by the transformation (4) as

$$\begin{aligned}
a_d(\boldsymbol{z}_d(t), \boldsymbol{z}_r(t)) &= L^q_{\boldsymbol{f}(\mathbf{z}_{orig}(t))}\boldsymbol{C}\mathbf{z}_{orig}(t)\mid_{\mathbf{z}_{orig}(t)=\boldsymbol{\phi}^{-1}(\boldsymbol{z}_d(t),\boldsymbol{z}_r(t))}\\
c(\boldsymbol{z}_d(t), \boldsymbol{z}_r(t)) &= L_{\boldsymbol{g}(\mathbf{z}_{orig}(t))}L^{q-1}_{\boldsymbol{f}(\mathbf{z}_{orig}(t))}\boldsymbol{C}\mathbf{z}_{orig}(t)\mid_{\mathbf{z}_{orig}(t)=\boldsymbol{\phi}^{-1}(\boldsymbol{z}_d(t),\boldsymbol{z}_r(t))}\\
b_k(\boldsymbol{z}_d(t), \boldsymbol{z}_r(t), u) &= L_{\boldsymbol{B}u}L^{k-1}_{\boldsymbol{f}(\mathbf{z}_{orig}(t))}\boldsymbol{C}\mathbf{z}_{orig}(t)\mid_{\mathbf{z}_{orig}(t)=\boldsymbol{\phi}^{-1}(\boldsymbol{z}_d(t),\boldsymbol{z}_r(t))};
\end{aligned} \tag{5}$$

the Frobenius Theorem implies that the system's description becomes

$$\begin{aligned}
\frac{d\boldsymbol{z}_c(t)}{dt} &= \bar{\boldsymbol{f}}(\boldsymbol{z}_c(t)) + \bar{\boldsymbol{g}}(\boldsymbol{z}_c(t), u(t)) + \Gamma(\boldsymbol{z}_c(t))\xi(t)\\
y(t) &= z_{d,1}(t)
\end{aligned} \tag{6}$$

where

$$\begin{aligned}
\bar{\boldsymbol{f}}(\boldsymbol{z}_c(t)) =& \mathrm{col}(z_{d,2}(t), \ldots, z_{d,q}(t), a_d(z_d(t), z_r(t)), \boldsymbol{a}_r(z_d(t), z_r(t)))\\
\bar{\boldsymbol{g}}(\boldsymbol{z}_c(t), u(t)) =& \mathrm{col}(b_1(\boldsymbol{z}_d(t), \boldsymbol{z}_r(t), u(t)), \ldots, b_{q-1}(\boldsymbol{z}_d(t), \boldsymbol{z}_r(t), u(t)),\\
& b_q(\boldsymbol{z}_d(t), \boldsymbol{z}_r(t), u(t)), \boldsymbol{b}_r(\boldsymbol{z}_d(t), \boldsymbol{z}_r(t), u(t)))\\
\boldsymbol{\Gamma}(\boldsymbol{z}_c(t)) =& \mathrm{col}(0, \ldots, 0, c(\boldsymbol{z}_d(t), \boldsymbol{z}_r(t)), \mathbf{0}_{1\times(n-q)}),
\end{aligned} \tag{7}$$

and $\boldsymbol{a}_r(\cdot)$ and $\boldsymbol{b}_r(\cdot)$ are vector fields of dimension $n-q$ obtained from transformation (4). The transformation (4) decomposes the system into two subsystems so that only $\boldsymbol{z}_d(t)$ is directly affected by the disturbances. More details on this transformation can be found in Isidori (1995).

Assumption 3: *The input terms in the transformed equations can be put into the form*

$$\begin{aligned} b_1(\boldsymbol{z}_d(t), \boldsymbol{z}_r(t), u(t)) &= b_1(y(t), u(t)) \\ b_2(\boldsymbol{z}_d(t), \boldsymbol{z}_r(t), u(t)) &= b_2(z_{d,2}(t), y(t), u(t)) \\ &\vdots \\ b_{q-1}(\boldsymbol{z}_d(t), \boldsymbol{z}_r(t), u(t)) &= b_{q-1}(z_{d,2}(t), \cdots, z_{d,q-1}(t), y(t), u(t)). \end{aligned}$$

Assumption 4: *The system with representation (1) and its corresponding transformed form (6) are bounded-input bounded-output (BIBO) stable for the output operator being the identity operator.*

The SMO design forces the system's states towards a sliding surface followed by stabilization of the error on the sliding surface. Some lemmas are required to establish convergence of the observer. First, Lipschitz continuity of the functions (5) follows from smoothness of the original system (1).

Lemma 1: *Let Assumption 1 be satisfied. There exist* $M_a, M_b, M_1, \cdots, M_q \in \mathbb{R}+$ *such that for every* $\boldsymbol{z}_c^T(t) = [\boldsymbol{z}_d^T(t), \boldsymbol{z}_r^T(t)]$ *and* $\hat{\boldsymbol{z}}_c^T(t) = [\hat{\boldsymbol{z}}_d^T(t), \hat{\boldsymbol{z}}_r^T(t)]$ *with* $\|\boldsymbol{z}_c(t) - \hat{\boldsymbol{z}}_c(t)\| \leq \epsilon_L$ *where* $\epsilon_L > 0$,

$$\begin{aligned} \|a_d(\boldsymbol{z}_d(t), \boldsymbol{z}_r(t)) - a_d(\hat{\boldsymbol{z}}_d(t), \hat{\boldsymbol{z}}_r(t))\| &\leq M_a \|\boldsymbol{z}_c(t) - \hat{\boldsymbol{z}}_c(t)\| \\ \|c(\boldsymbol{z}_d(t), \boldsymbol{z}_r(t)) - c(\hat{\boldsymbol{z}}_d(t), \hat{\boldsymbol{z}}_r(t))\| &\leq M_c \|\boldsymbol{z}_c(t) - \hat{\boldsymbol{z}}_c(t)\| \\ \|b_k(\boldsymbol{z}_d(t), \boldsymbol{z}_r(t), u(t)) - b_k(\hat{\boldsymbol{z}}_d(t), \hat{\boldsymbol{z}}_r(t), u(t))\| &\leq M_k \|\boldsymbol{z}_c(t) - \hat{\boldsymbol{z}}_c(t)\| \end{aligned} \tag{8}$$

for $k = 1, \ldots, q$.

Proof: The proof followed from Assumption 1, the transformation $\boldsymbol{z}_c(t) = [\boldsymbol{z}_d^T(t), \boldsymbol{z}_r^T(t)]^T = \boldsymbol{\phi}(\mathbf{z}_{orig}(t))$ given by (4) being a diffeomorphism, and the Mean Value Theorem. □

Now, a method for estimation of the undisturbed nonlinear system will be combined with a SMO to obtain an observer for the disturbed system. Define the state vector $\tilde{\boldsymbol{z}}_c^T(t) = [\tilde{\boldsymbol{z}}_d^T(t), \tilde{\boldsymbol{z}}_r^T(t)]$; the undisturbed system is defined as

$$\begin{aligned} \frac{d\tilde{\boldsymbol{z}}_c(t)}{dt} &= \bar{\boldsymbol{f}}(\tilde{\boldsymbol{z}}_c(t)) + \bar{\boldsymbol{g}}(\tilde{\boldsymbol{z}}_c(t), u(t)) \\ y(t) &= \tilde{z}_{d,1}(t) \end{aligned} \tag{9}$$

The representation (9) is assumed to be detectable in the sense that an exponentially convergent observer can be designed for this system.

Define $\tilde{\mathbf{e}}(t) = \tilde{\boldsymbol{z}}_c(t) - \hat{\boldsymbol{z}}_c(t) = [\tilde{e}_1(t), \cdots, \tilde{e}_q(t), \tilde{e}_{q+1}(t), \cdots, \tilde{e}_n(t)]^T$ and $\tilde{e}_1(t) = \tilde{z}_{d,1}(t) - \hat{z}_{d,1}(t)$; indicate the observer gain by $\boldsymbol{K}(\cdot)$. The observer dynamics using the transformed equations (6) become

$$\frac{d\hat{\boldsymbol{z}}_c(t)}{dt} = \bar{\boldsymbol{f}}(\hat{\boldsymbol{z}}_c(t)) + \bar{\boldsymbol{g}}(\hat{\boldsymbol{z}}_c(t), u(t)) + \boldsymbol{K}(\hat{\boldsymbol{z}}_c(t), \tilde{e}_1(t)) \tag{10}$$

where $\boldsymbol{K}^T(\hat{\boldsymbol{z}}_c(t), \tilde{e}_1(t)) = [K_1(\hat{\boldsymbol{z}}_c(t), \tilde{e}_1(t)), \ldots, K_n(\hat{\boldsymbol{z}}_c(t), \tilde{e}_1(t))]$ is designed such that

$$\| \boldsymbol{K}(\hat{\boldsymbol{z}}_c(t), \tilde{e}_1(t)) \| \leq k \| \tilde{e}_1(t) \| . \tag{11}$$

If the disturbance $\xi = 0$ the error dynamics take the form

$$\frac{d\tilde{\boldsymbol{e}}(t)}{dt} = \bar{\boldsymbol{f}}(\tilde{\boldsymbol{z}}_c(t)) - \bar{\boldsymbol{f}}(\hat{\boldsymbol{z}}_c(t)) + \bar{\boldsymbol{g}}(\tilde{\boldsymbol{z}}_c(t), u(t)) - \bar{\boldsymbol{g}}(\hat{\boldsymbol{z}}_c(t), u(t)) - \boldsymbol{K}(\hat{\boldsymbol{z}}_c(t), \tilde{e}_1(t)). \tag{12}$$

Assumption 5: *Let the observer dynamics and its corresponding error dynamics be given by equations (10) and (12), respectively. There exists a continuously differentiable Lyapunov function* $V : \mathcal{D} \to \mathbb{R}$ *such that*

$$\beta_1 \parallel \tilde{\mathbf{e}}(t) \parallel^2 \leq V(\tilde{\mathbf{e}}(t)) \leq \beta_2 \parallel \tilde{\mathbf{e}}(t) \parallel^2 \tag{13}$$

$$\| \frac{\partial V(\tilde{\mathbf{e}}(t))}{\partial \tilde{\mathbf{e}}(t)} \| \leq \beta_4 \|\tilde{\mathbf{e}}(t)\| \tag{14}$$

for some $\beta_1, \beta_2, \beta_3, \beta_4 > 0$ *and along trajectories*

$$\frac{dV(\tilde{\boldsymbol{e}}(t))}{dt} = V_0(\tilde{\boldsymbol{e}}(t)) \leq -\beta_3 \parallel \tilde{\boldsymbol{e}}(t) \parallel^2 \ . \tag{15}$$

If the disturbance $\xi \neq 0$, the observer is modified by adding some sliding mode terms. Combining an exponential convergent nonlinear observer satisfying Assumption 5 with a sliding mode term reduces the effect of chattering associated with some sliding mode observers.

Define $e_1(t) = z_{d,1}(t) - \hat{z}_{d,1}(t)$ where $\hat{\boldsymbol{z}}_c^T(t) = [\hat{\boldsymbol{z}}_d^T(t), \hat{\boldsymbol{z}}_r^T(t)]$ is the observer state vector, $\bar{e}_1(t) = e_1(t)$, and $\bar{e}_k(t) = (\lambda_{k-1}\,\mathrm{sign}(\bar{e}_{k-1}(t)))_{eq}$ for $k = 2 \cdots q$ where $(\lambda_{k-1}\,\mathrm{sign}(\bar{e}_{k-1}(t)))_{eq}$ are equivalent signals obtained by low pass filtering the signals $\lambda_{k-1}\,\mathrm{sign}(\bar{e}_{k-1}(t))$ with an antipeaking structure introduced in Drakunov (1992); this filter is designed to avoid peaking phenomenon in a way that the information regarding the observation error $e_{k-1}(t)$ is not used till the sliding manifold $e_{k-1}(t) = 0$ assigned with this information is reached. In other words, $\bar{e}_k(t)$ is set to zero till the sliding manifolds $e_{k-1}(t) = 0$ are reached one by one in a recursive manner. The observer dynamics are

$$\begin{aligned}
\frac{d\hat{z}_{d,1}(t)}{dt} &= \hat{z}_{d,2}(t) + b_1(y(t), u(t)) + K_1(\hat{\boldsymbol{z}}(t), e_1(t)) + \lambda_1\,\mathrm{sign}(e_1(t)) \\
&\vdots \\
\frac{d\hat{z}_{d,q-1}(t)}{dt} &= \hat{z}_{d,q}(t) + b_{q-1}(\hat{z}_{d,2}(t), \cdots, \hat{z}_{d,q-1}(t), y(t), u(t)) + K_2(\hat{\boldsymbol{z}}(t), e_1(t)) + \lambda_{q-1}\,\mathrm{sign}(\bar{e}_{q-1}(t)) \\
\frac{d\hat{z}_{d,q}(t)}{dt} &= a_d(\hat{\boldsymbol{z}}_d(t), \hat{\boldsymbol{z}}_r(t)) + b_q(\hat{\boldsymbol{z}}_d(t), \hat{\boldsymbol{z}}_r(t), u(t)) + K_q(\hat{\boldsymbol{z}}(t), e_1(t)) + \lambda_q\,\mathrm{sign}(\bar{e}_q(t)) \\
\frac{d\hat{\boldsymbol{z}}_r(t)}{dt} &= \boldsymbol{a}_r(\hat{\boldsymbol{z}}_d(t), \hat{\boldsymbol{z}}_r(t)) + \boldsymbol{b}_r(\hat{\boldsymbol{z}}_d(t), \hat{\boldsymbol{z}}_r(t), u(t)) + K_{q+1:n}(\hat{\boldsymbol{z}}_c(t), e_1(t)).
\end{aligned} \tag{16}$$

This observer can also be written

$$\frac{d\hat{\boldsymbol{z}}_c(t)}{dt} = \bar{\boldsymbol{f}}(\hat{\boldsymbol{z}}_c(t)) + \bar{\boldsymbol{g}}(\hat{\boldsymbol{z}}_c(t), u(t)) + \boldsymbol{K}(\hat{\boldsymbol{z}}_c(t), e_1(t)) + \boldsymbol{u}_r(t) \tag{17}$$

where

$$\boldsymbol{u}_r(t) = \mathrm{col}(\lambda_1\,\mathrm{sign}(e_1(t)), \ldots, \lambda_q\,\mathrm{sign}(\bar{e}_q(t)), \mathbf{0}_{1\times(n-q)}).$$

Lemma 2: *Let Assumptions 1, 4, and 5 be satisfied. The estimation error provided by the observer (16) is bounded on every time interval* $[t_0, t_f]$ *where* $t_f > 0$. *The bound is given by*

$$\|\boldsymbol{e}(t)\| \leq \max((\beta_4 M_d)/\beta_3, \sqrt{V(\boldsymbol{e}(0))/\beta_1}) \tag{18}$$

where β_3, β_4, *and* $V(\cdot)$ *are defined in Assumption 5, and*

$$M_d = M_0 + \sup_{t\in[t_0,t_f]} (\|\boldsymbol{u}_r(t)\|) \leq M_0 + \sqrt{q}\max_i(\lambda_i) \tag{19}$$

with $M_0 > 0$ *representing the upper bound of* $\|\boldsymbol{\Gamma}(\boldsymbol{z}_c(t))\xi(t)\|$.

Proof: Define the error vector $\boldsymbol{e}(t) = \boldsymbol{z}_c(t) - \hat{\boldsymbol{z}}_c(t)$; the error dynamics can be obtained from equations (6) and (17) as

$$\begin{aligned}\frac{d\boldsymbol{e}(t)}{dt} &= \bar{\boldsymbol{f}}(\boldsymbol{z}_c(t)) - \bar{\boldsymbol{f}}(\hat{\boldsymbol{z}}_c(t)) + \bar{\boldsymbol{g}}(\boldsymbol{z}_c(t), u(t)) - \bar{\boldsymbol{g}}(\hat{\boldsymbol{z}}_c(t), u(t)) \\ &\quad - \boldsymbol{K}(\hat{\boldsymbol{z}}_c(t), e_1(t)) + \boldsymbol{\Gamma}(\boldsymbol{z_c(t)})\xi(t) - \boldsymbol{u}_r(t)\,.\end{aligned} \tag{20}$$

Consider a continuously differentiable Lyapunov function $V(\cdot)$ satisfying Assumption 5. Along trajectories,

$$\frac{dV(\boldsymbol{e}(t))}{dt} = V_0(\boldsymbol{e}(t)) + \frac{\partial V(\boldsymbol{e}(t))}{\partial \boldsymbol{e}(t)}\left(\boldsymbol{\Gamma}(\boldsymbol{z}_c(t))\xi(t) - \boldsymbol{u}_r(t)\right);$$

employing inequalities (14) and (15) leads to

$$\frac{dV(\boldsymbol{e}(t))}{dt} \leq -\beta_3\|\boldsymbol{e}(t)\|^2 + \beta_4\|\boldsymbol{\Gamma}(\boldsymbol{z}_c(t))\xi(t) - \boldsymbol{u}_r(t)\|\|\boldsymbol{e}(t)\|. \tag{21}$$

From the definition of $\boldsymbol{\Gamma}(\boldsymbol{z}_c(t))$, equation (7), Lemma 1, Assumption 4, and the boundedness of the vector $\boldsymbol{u}_r(t)$ and unknown input $\xi(t)$, it can be concluded that

$$\|\boldsymbol{\Gamma}(\boldsymbol{z}_c(t))\xi(t) - \boldsymbol{u}_r(t)\| \leq M_d$$

where $M_d > 0$ is defined in (19). Therefore,

$$\frac{dV(\boldsymbol{e}(t))}{dt} \leq -\beta_3\|\boldsymbol{e}(t)\|^2 + \beta_4 M_d\|\boldsymbol{e}(t)\|. \tag{22}$$

If $\|\boldsymbol{e}(t)\| < \frac{\beta_4 M_d}{\beta_3}$ the error vector is of course bounded and the proof is complete. Suppose then that $\|\boldsymbol{e}(t)\| \geq \frac{\beta_4 M_d}{\beta_3}$. From inequalities (13) and (22), this implies that

$$\frac{dV(\boldsymbol{e}(t))}{dt} \leq 0, \quad \text{and} \quad \|\boldsymbol{e}(t)\| \leq \sqrt{\frac{V(\boldsymbol{e}(t))}{\beta_1}} \leq \sqrt{\frac{V(\boldsymbol{e}(0))}{\beta_1}}.$$

In this case, the error vector is bounded by (18) □

Theorem 1: *Suppose that Assumptions 1-4 hold and also the error dynamics for the undisturbed system ($\xi = 0$) defined in (12) satisfy Assumption 5 with*

$$\beta_3 > \beta_4(1 + M_a + M_q)$$

where $M_a, M_q > 0$ are defined in Lemma 1. Then there exists $\lambda_1, \cdots, \lambda_q > 0$ such that the modified sliding mode observer (16) provides an exponential convergence of the estimation vector $\hat{\boldsymbol{z}}_c(t)$ to the state vector $\boldsymbol{z}_c(t)$.

Proof: If the disturbance input $\xi(t)$ is zero, the result follows trivially from the assumptions. Consider then a non-zero disturbance term $\xi(t) \neq 0$. The proof involves several steps.

Step 1: This step is along the lines of the proof of (Xiong and Saif, 2001, Theorem 1). Let $\boldsymbol{e}(t) = [\boldsymbol{e}_d^T(t), \boldsymbol{e}_r^T(t)]^T = \boldsymbol{z}_c(t) - \hat{\boldsymbol{z}}_c(t)$ where $\boldsymbol{e}_d(t) = [e_1(t), \ldots, e_q(t)]^T$, and $\boldsymbol{e}_q(t) = [e_{q-1}(t), \ldots, e_n(t)]^T$. The error dynamics of the vector $\boldsymbol{e}_d(t)$ are expanded as

$$\frac{de_1(t)}{dt} = e_2(t) - K_1(\hat{\boldsymbol{z}}_c(t), e_1(t)) - \lambda_1 \operatorname{sign}(e_1(t)) \tag{23}$$

$$\frac{de_2(t)}{dt} = e_3(t) + b_2(z_{d,2}(t), y(t), u(t)) - b_{q-1}(\hat{z}_{d,2}(t), y(t), u(t)) \tag{24}$$

$$- K_2(\hat{\boldsymbol{z}}_c(t), e_1(t)) - \lambda_2 \operatorname{sign}(\bar{e}_2(t)) \tag{25}$$

$$\vdots$$

$$\frac{de_{q-1}(t)}{dt} = e_q(t) + b_{q-1}(z_{d,2}(t), \ldots, z_{d,q-1}(t), y(t), u(t)) - b_{q-1}(\hat{z}_{d,2}(t), \ldots, \hat{z}_{d,q-1}(t), y(t), u(t))$$
$$- K_{q-1}(\hat{\boldsymbol{z}}_c(t), e_1(t)) - \lambda_{q-1} \operatorname{sign}(\bar{e}_{q-1}(t)) \tag{26}$$

$$\frac{de_q(t)}{dt} = a_d(\boldsymbol{z}_d(t), \boldsymbol{z}_r(t)) - a_d(\hat{\boldsymbol{z}}_d(t), \hat{\boldsymbol{z}}_r(t)) + b_q(\boldsymbol{z}_d(t), \boldsymbol{z}_r(t), u(t)) - b_q(\hat{\boldsymbol{z}}_d(t), \hat{\boldsymbol{z}}_r(t), u(t))$$
$$- K_q(\hat{\boldsymbol{z}}_c(t), e_1(t)) + c(\boldsymbol{z}_d(t), \boldsymbol{z}_r(t))\xi(t) - \lambda_q \operatorname{sign}(\bar{e}_q(t)). \tag{27}$$

Consider the first dynamical equation (23) of the error dynamics. Defining the Lyapunov function $V_1(e_1) = 1/2e_1^2$,

$$\frac{dV_1(e_1)}{dt} = e_1 e_2 - e_1 K_1(\hat{z}_c, e_1) - \lambda_1 |e_1|. \tag{28}$$

From (28) and inequality (11), it is concluded that

$$\frac{dV_1(e_1)}{dt} \leq (|e_2| + k|e_1| - \lambda_1)|e_1|. \tag{29}$$

The estimation error is bounded by Lemma 2 in two possible ways; in (18), if $\sqrt{V(\boldsymbol{e}(0))/\beta_1} \geq \beta_4 M_d/\beta_3$, the error vector $\boldsymbol{e}$ is bounded by $\sqrt{V(\boldsymbol{e}(0))/\beta_1}$, so $(|e_2| + k|e_1|)$ has an upper bound. In this case, choose $\lambda_1 > (1 + k)\sqrt{V(\boldsymbol{e}(0))/\beta_1}$. Otherwise, the upper bound is $\beta_4 M_d/\beta_3$ where M_d is defined by (19) in which, by definition, $\boldsymbol{u}_r = \operatorname{col}(\lambda_1 \operatorname{sign}(e_1), 0, \ldots, 0)$ and $\|\boldsymbol{u}_r\| = \lambda_1$ since the sliding manifold $e_1 = 0$ has not reached yet. In (29), let $|e_2|$ be replaced by this upper bound; it is derived that

$$\frac{dV_1(e_1)}{dt} \leq \Big(\frac{\beta_4 M_0}{\beta_3} - (1 - \frac{\beta_4}{\beta_3})\lambda_1 + k|e_1|\Big)|e_1|. \tag{30}$$

By assumption, $\beta_4/\beta_3 < 1$. Furthermore, by continuity $|e_1| < L_1$ for some $L_1 > 0$ on a finite time interval $[t_0, t_0 + \epsilon_t]$ for some $\epsilon_t > 0$; choose $\lambda_1 > \beta_3/(\beta_3 - \beta_4)(\beta_4 M_0/\beta_3 + kL_1)$.

Following both possibilities for choosing λ_1, define

$$\beta_5 = \lambda_1 - \max\left(\frac{(1+k)\sqrt{V(\boldsymbol{e}(0))}}{\beta_1}, \frac{\beta_3}{\beta_3 - \beta_4}(\frac{\beta_4 M_0}{\beta_3} + kL_1)\right)$$

and note $\beta_5 > 0$. Thus, inequality (29) and (30) become

$$\frac{dV_1(e_1)}{dt} \leq -\beta_5 |e_1|. \tag{31}$$

From this inequality, it is obvious that $|e_1|$ is decreasing; thus, $\epsilon_t > 0$ can be chosen arbitrarily large, and (31) is true for every $t \geq t_0$. From (31), it is also concluded that the system reaches the switching surface $e_1 = 0$ after a finite time t_1. After this ideal sliding motion takes place, $e_1 = 0$ and $de_1/dt = 0$ for $t > t_1$. The second equation (24) becomes

$$\frac{de_2}{dt} = e_3 + b_2(z_{d,2}, y, u) - b_{q-1}(\hat{z}_{d,2}, y, u) - K_2(\hat{\boldsymbol{z}}_c, e_1) - \lambda_2 \operatorname{sign}(e_2).$$

Furthermore, for $t > t_1$, $\boldsymbol{u}_r = \operatorname{col}(e_2, \lambda_2 \operatorname{sign}(e_2), 0, \ldots, 0)$ till the system reaches the switching surface $e_2 = 0$ by definition. Followed by the same procedure as before, let $|e_2| \leq L_2$ on $[t_1, t_1 + \epsilon_t]$; Given Lemma 2, inequalities (11) and (8) as well as the boundedness of e_1 and e_2, one can choose

$$\lambda_2 > \max\left(\frac{(1+k+M_1)\sqrt{V(\boldsymbol{e}(0))}}{\beta_1}, \frac{\beta_3}{\beta_3 - \beta_4}(\frac{\beta_4(M_0 + L_2)}{\beta_3} + kL_1 + M_1 L_2)\right)$$

for which, as was shown before for $|e_1|$, $|e_2|$ is decreasing; thus, $\epsilon_t > 0$ can be chosen arbitrarily and the system reaches the switching surface $e_2 = 0$ after a finite time $t_2 > t_1$. Following the same reasoning implies that after finite time $T > t_q > \ldots > t_2 > t_1$ the system reaches the sliding surfaces $e_1 = 0, \ldots, e_q = 0$ one by one.

Step 2: Once the motion is along the intersection of the sliding surfaces, $e_1 = 0, \ldots, e_q = 0$, the discontinuous vector $\boldsymbol{u}_r$ in equation (17) can be replaced by its equivalent smooth counterpart Edwards and Spurgeon (1998)

$$\begin{aligned} \boldsymbol{u}_{eq} &= \operatorname{col}(e_2, \ldots, e_q, c_d(\boldsymbol{z}_d), \boldsymbol{z}_r, u, \xi), \boldsymbol{0}_{(n-q)\times 1}) \\ c_d(\boldsymbol{z}_d), \boldsymbol{z}_r, u, \xi) &= a_d(\boldsymbol{z}_d, \boldsymbol{z}_r) - a_d(\boldsymbol{z}_d, \hat{\boldsymbol{z}}_r) + \\ &\quad b_q(\boldsymbol{z}_d, \boldsymbol{z}_r, u) - b_q(\boldsymbol{z}_d, \hat{\boldsymbol{z}}_r, u) + c(\boldsymbol{z}_d, \boldsymbol{z}_r)\xi \end{aligned} \tag{32}$$

where $\boldsymbol{u}_{eq}$ forces the system's motion to stay along the intersection of some sliding surfaces; then, the error dynamics of the system take the form

$$\frac{d\boldsymbol{e}}{dt} = \bar{\boldsymbol{f}}(\boldsymbol{z}_c) - \bar{\boldsymbol{f}}(\hat{\boldsymbol{z}}_c) + \bar{\boldsymbol{g}}(\boldsymbol{z}_c, u) - \bar{\boldsymbol{g}}(\hat{\boldsymbol{z}}_c, u) - \boldsymbol{K}(\hat{\boldsymbol{z}}_c, e_1) + \boldsymbol{\Gamma}(\boldsymbol{z}_c)\xi - \boldsymbol{u}_{eq}. \tag{33}$$

From equation (32) and the inequalities (8),

$$\|\boldsymbol{\Gamma}(\boldsymbol{z}_c)\xi - \boldsymbol{u}_{eq}\| \leq (1 + M_a + M_q)\|\boldsymbol{e}\|. \tag{34}$$

Step 3: The observer $\boldsymbol{K}(\hat{\boldsymbol{z}}_c, e_1)$ was proven in Lemma 2 to provide a bounded error even for a system with disturbances. In sliding mode, which occurs after finite time, the error dynamics are given by equation (33). Differentiating the Lyapunov function $V(\cdot)$ satisfying Assumption 5 leads to

$$\frac{dV(\boldsymbol{e})}{dt} = V_0(\boldsymbol{e}) + \frac{\partial V(\boldsymbol{e})}{\partial \boldsymbol{e}}(\boldsymbol{\Gamma}(\boldsymbol{z}_c)\xi - \boldsymbol{u}_{eq}). \tag{35}$$

Inequalities (14), (15), and (34) imply that

$$\frac{dV(\boldsymbol{e})}{dt} \leq -\beta_3\|\boldsymbol{e}\|^2 + \beta_4(1 + M_a + M_q)\|\boldsymbol{e}\|^2 \,. \tag{36}$$

Since $\beta_3 > \beta_4(1 + M_a + M_q)$, for some $\beta_6 = \beta_3 - \beta_4(1 + M_a + M_q) > 0$

$$\frac{dV(\boldsymbol{e})}{dt} \leq -\beta_6\|\boldsymbol{e}\|^2 \tag{37}$$

and the estimation error $\boldsymbol{e}$ goes to zero exponentially. □

Theorem 1 shows that an exponentially convergent observer for the undisturbed nonlinear system can be combined with the sliding mode observer. The result is an exponentially convergent observer in the presence of disturbances coming from an unknown input. A number of estimation methods can be used for the undisturbed systems. In the simulations below, the EKF is used.

There are two ways of handling the transformation of the observer states to the original coordinates: finding the state space representation of the observer in the original coordinates, or transforming the estimated state back into the original coordinates. Direct transformation of the estimated state back into the original coordinates is a practical choice when the observer dynamics can be sampled for its solution. In this paper, the observer state in the original coordinates is obtained by $\hat{\boldsymbol{z}}_{orig} = \boldsymbol{\phi}^{-1}(\hat{\boldsymbol{z}}_c)$.

3. Observer design for distributed parameter systems

Consider a distributed parameter system with state in a separable Hilbert space $\mathcal{H}$ and model

$$\begin{aligned} \frac{\partial \boldsymbol{z}}{\partial t} &= \boldsymbol{\mathcal{F}}(\boldsymbol{z}) + \boldsymbol{\mathcal{B}}u(t) + \boldsymbol{\mathcal{G}}(\boldsymbol{z})\xi(t), \qquad \boldsymbol{z}(0,\boldsymbol{x}) = \boldsymbol{z}_0 \in \mathcal{H} \\ y(t) &= \mathcal{C}\boldsymbol{z} \end{aligned} \tag{38}$$

where $\boldsymbol{z} \in \mathcal{H}$, $\boldsymbol{x} \in \mathbb{R}^m$ is the spatial variable, $\boldsymbol{\mathcal{F}}(\cdot) : \mathcal{D}(\boldsymbol{\mathcal{F}}) \subset \mathcal{H} \to \mathcal{H}$ is a nonlinear operator, $\boldsymbol{\mathcal{B}} : \mathbb{R} \to \mathcal{H}$ is the input operator and bounded, $\boldsymbol{\mathcal{G}}(\cdot) : \mathbb{R} \to \mathcal{H}$ is the disturbance operator, $u \in \mathbb{R}$ is the input signal, $\xi \in \mathbb{R}$ is the disturbance input, $y \in \mathbb{R}$ is the output signal, and $\mathcal{C} : \mathcal{H} \to \mathbb{R}$ is the output operator and linear bounded.

Let $\{\boldsymbol{v}_i\}_{i=1}^{\infty}$ be a basis for $\mathcal{H}$. Now, define the finite-dimensional subspace

$$\mathcal{H}_M = \text{span}\{\boldsymbol{v}_k, k = 1 \ldots M\}.$$

The orthogonal projection of $\mathcal{H}$ onto $\mathcal{H}_M$ is

$$\boldsymbol{\mathcal{P}}_M \boldsymbol{z} = \sum_{i=1}^{M} z_i \boldsymbol{v}_i \tag{39}$$

for $\boldsymbol{z} \in \mathcal{H}$ and $z_i \in \mathbb{R}$. Let the state vector be decomposed into two parts $\boldsymbol{z} = \boldsymbol{z}_M + \boldsymbol{z}_M^c$ with $\boldsymbol{z}_M = \boldsymbol{\mathcal{P}}_M \boldsymbol{z}$, $\boldsymbol{z}_M^c = (\boldsymbol{\mathcal{I}} - \boldsymbol{\mathcal{P}}_M)\boldsymbol{z}$.

The projection (39) can be used to approximate the system (38) by a finite-dimensional system of the form

$$\begin{aligned}\frac{\partial \bar{\boldsymbol{z}}_M}{\partial t} &= \boldsymbol{\mathcal{F}}_M(\bar{\boldsymbol{z}}_M) + \boldsymbol{\mathcal{B}}_M u(t) + \boldsymbol{\mathcal{G}}_M(\bar{\boldsymbol{z}}_M)\xi(t) \\ y(t) &= \boldsymbol{\mathcal{C}}\bar{\boldsymbol{z}}_M.\end{aligned} \tag{40}$$

The state variables $\bar{\boldsymbol{z}}_M$ and $\boldsymbol{z}_M$ are different: the state $\boldsymbol{z}_M$ is the projection of the solution to (38) onto $\mathcal{H}_M$ while $\bar{\boldsymbol{z}}_M$ satisfies the finite-dimensional system (40). An ODE representation on $\mathbb{R}^M$ equivalent to (40) can be obtained via multiplying both sides of (40) by $\boldsymbol{v}_i$ for $i = 1 \dots M$ in the sense of $\mathcal{H}$ inner product $(\cdot,\cdot)_{\mathcal{H}}$. This leads to

$$\begin{aligned}\frac{d\mathbf{z}_{orig,M}}{dt} &= \boldsymbol{f}_M(\mathbf{z}_{orig,M}) + \boldsymbol{B}_M u(t) + \boldsymbol{g}_M(\mathbf{z}_{orig,M})\xi(t) \\ y &= \boldsymbol{C}_M \mathbf{z}_{orig,M}\end{aligned} \tag{41}$$

where $\boldsymbol{f}_M(\cdot)$ and $\boldsymbol{g}_M(\cdot)$ are functions defined on $\mathbb{R}^M$ and $\boldsymbol{B}_M$ is a column matrix of dimension M.

The observer dynamics are composed of a copy of the system approximate dynamics (41) with $N \le M$ and a filtering feedback operator. Define

$$\mathbf{z}_{orig,N} = \mathrm{col}(\bar{z}_1, \bar{z}_2, \dots, \bar{z}_N), \quad \mathbf{z}^c_{orig,N} = \mathrm{col}(\bar{z}_{N+1}, \bar{z}_{N+2}, \dots, \bar{z}_M).$$

The system (41) is rewritten as

$$\begin{aligned}\frac{d\mathbf{z}_{orig,N}}{dt} &= \boldsymbol{f}_N(\mathbf{z}_{orig,N}) + \boldsymbol{B}_N u(t) + \boldsymbol{g}_N(\mathbf{z}_{orig,N})\xi(t) + \boldsymbol{h}_N(\mathbf{z}_{orig,N}, \mathbf{z}_{orig,M}) \\ \frac{d\mathbf{z}^c_{orig,N}}{dt} &= \boldsymbol{f}^c_N(\mathbf{z}_{orig,M}) + \boldsymbol{B}^c_N u(t) + \boldsymbol{g}^c_N(\mathbf{z}_{orig,M})\xi(t) \\ y &= \boldsymbol{C}_M \mathbf{z}_{orig,M}\end{aligned} \tag{42}$$

where

$$\boldsymbol{h}_N(\mathbf{z}_{orig,N}, \mathbf{z}_{orig,M}) = \boldsymbol{f}_N(\mathbf{z}_{orig,M}) - \boldsymbol{f}_N(\mathbf{z}_{orig,N}) + (\boldsymbol{g}_N(\mathbf{z}_{orig,M}) - \boldsymbol{g}_N(\mathbf{z}_{orig,N}))\xi(t).$$

Next, the following change of coordinate

$$\boldsymbol{z}_{c,M} = \begin{bmatrix}\boldsymbol{z}_{c,N} \\ \boldsymbol{z}^c_{c,N}\end{bmatrix} = \boldsymbol{T}_M(\mathbf{z}_{orig,M}) = \begin{bmatrix}\boldsymbol{\phi}_N(\mathbf{z}_{orig,N}) \\ \mathbf{z}^c_{orig,N}\end{bmatrix}$$

is applied wherein $\boldsymbol{\phi}_N(\mathbf{z}_{orig,N})$ is defined as in (4) with $\boldsymbol{f}(\cdot)$ and $\boldsymbol{g}(\cdot)$ respectively replaced by $\boldsymbol{f}_N(\cdot)$ and $\boldsymbol{g}_N(\cdot)$.

In the new coordinates, the system takes the form

$$\begin{aligned}\frac{d\boldsymbol{z}_{c,N}}{dt} &= \bar{\boldsymbol{f}}_N(\boldsymbol{z}_{c,N}) + \bar{\boldsymbol{g}}_N(\boldsymbol{z}_{c,N}, u(t)) + \boldsymbol{\Gamma}_N(\boldsymbol{z}_{c,N})\xi(t) + \bar{\boldsymbol{h}}_N(\boldsymbol{z}_{c,N}, \boldsymbol{z}_{c,N}) \\ \frac{d\mathbf{z}^c_{orig,N}}{dt} &= \boldsymbol{f}^c_N(\boldsymbol{z}_{c,M}) + \boldsymbol{B}^c_N u(t) + \boldsymbol{g}^c_N(\boldsymbol{z}_{c,M})\xi(t) \\ y &= [1, 0, \dots, 0]\boldsymbol{z}_{c,M}\end{aligned} \tag{43}$$

where $\bar{\boldsymbol{f}}_N(\cdot)$, $\bar{\boldsymbol{g}}_N(\cdot)$, $\boldsymbol{\Gamma}_N(\cdot)$, and $\bar{\boldsymbol{h}}_N(\cdot)$ are transformed forms of $\boldsymbol{f}_N(\cdot)$, $\boldsymbol{B}_N$, $\boldsymbol{g}_N(\cdot)$, and $\boldsymbol{h}_N(\cdot)$ through mapping (4). Note that $\bar{\boldsymbol{f}}_N(\cdot)$, $\bar{\boldsymbol{g}}_N(\cdot)$, and $\boldsymbol{\Gamma}_N(\cdot)$ have the same structures as but different dimensions from $\bar{\boldsymbol{f}}(\cdot)$, $\bar{\boldsymbol{g}}(\cdot)$, and $\boldsymbol{\Gamma}(\cdot)$ since the mappings $\boldsymbol{\phi}_N(\cdot)$ and $\boldsymbol{\phi}(\cdot)$ are constructed based on the same logic.

Define $\hat{\boldsymbol{z}}_{c,N} = [\hat{z}_{c,1}, \hat{z}_{c,2}, \ldots, \hat{z}_{c,N}]^T$. The general observer dynamics have the form

$$\frac{d\hat{\boldsymbol{z}}_{c,N}}{dt} = \bar{\boldsymbol{f}}_N(\hat{\boldsymbol{z}}_{c,N}) + \bar{\boldsymbol{g}}_N(\hat{\boldsymbol{z}}_{c,N}, u(t)) + \boldsymbol{K}_N(\hat{\boldsymbol{z}}_{c,N}, y - \hat{z}_{c,1}) + \boldsymbol{u}_{r,N} \tag{44}$$

where $\boldsymbol{K}_N(\cdot)$ is the filtering gain and $\boldsymbol{u}_{r,N}$ is defined in the same way as $\boldsymbol{u}_r$ in (17) for $n = N$. Define $\boldsymbol{e}_N = [e_{N,1}, e_{N,2}, \ldots, e_{N,N}]^T = \boldsymbol{z}_{c,N} - \hat{\boldsymbol{z}}_{c,N}$. The error dynamics become

$$\begin{aligned} \frac{d\boldsymbol{e}_N}{dt} &= \bar{\boldsymbol{f}}_N(\boldsymbol{z}_{c,N}) - \bar{\boldsymbol{f}}_N(\hat{\boldsymbol{z}}_{c,N}) + \bar{\boldsymbol{g}}_N(\boldsymbol{z}_{c,N}, u(t)) - \bar{\boldsymbol{g}}_N(\hat{\boldsymbol{z}}_{c,N}, u(t)) \\ &\quad - \boldsymbol{K}_N(\hat{\boldsymbol{z}}_{c,N}, e_{N,1}) + \boldsymbol{\Gamma}_N(\boldsymbol{z}_{c,N})\xi(t) - \boldsymbol{u}_{r,N} + \bar{\boldsymbol{h}}_N(\boldsymbol{z}_{c,N}, \boldsymbol{z}_{c,M}) \\ \frac{d\mathbf{z}^c_{orig,N}}{dt} &= \boldsymbol{f}^c_N(\boldsymbol{z}_{c,M}) + \boldsymbol{B}^c_N u(t) + \boldsymbol{g}^c_N(\boldsymbol{z}_{c,M})\xi(t). \end{aligned} \tag{45}$$

Lemma 3: *Suppose that Assumptions 1-3 hold for $\boldsymbol{f}(\cdot) = \boldsymbol{f}_N(\cdot)$, $\boldsymbol{g}(\cdot) = \boldsymbol{g}_N(\cdot)$, $n = N$, and $q = 1$, and the system (42) satisfies Assumption 4. Furthermore, for $\boldsymbol{z}^c_{orig,N} = 0$, $u_{r,N} = 0$, and $\xi(t) = 0$, let the error dynamics (45) satisfy Assumption 5 with $n = N$. Furthermore, suppose that $\bar{\boldsymbol{h}}_N(\boldsymbol{z}_{c,N}, \boldsymbol{z}_{c,M})$ is bounded for every N. In other words,*

$$\|\bar{\boldsymbol{h}}_N(\boldsymbol{z}_{c,N}, \boldsymbol{z}_{c,M})\| \leq M_h$$

for some $M_h > 0$. The state estimate provided by the observer (44) is bounded.

Proof: The proof is given in the appendix. □

Boundedness of the estimation error is provided by the following theorem.

Theorem 2: *Suppose that Assumptions 1-3 hold for $\boldsymbol{f}(\cdot) = \boldsymbol{f}_N(\cdot)$, $\boldsymbol{g}(\cdot) = \boldsymbol{g}_N(\cdot)$, $n = N$, and $q = 1$, and the system (42) satisfies Assumption 4. Furthermore, for $\boldsymbol{z}^c_{orig,N} = 0$, $u_{r,N} = 0$, and $\xi(t) = 0$, let the error dynamics (45) satisfy Assumption 5 with $n = N$ and*

$$\beta_3 > \beta_4(1 + M_a + M_q)$$

where $M_a, M_q > 0$ are defined in Lemma 1. Suppose that $\bar{\boldsymbol{h}}_N(\boldsymbol{z}_{c,N}, \boldsymbol{z}_{c,M})$ is uniformly bounded for every N. Then there exists $\lambda_1, \cdots, \lambda_q > 0$ such that the approximate observer (44) provides bounded estimation error compared with the higher order approximated system (43). More precisely, defining $\beta_6 = \beta_3 - \beta_4(1 + M_a + M_q)$,

$$\|\boldsymbol{e}\| \leq \|\boldsymbol{e}_N\| + \|\boldsymbol{z}^c_{orig,N}\| \leq \frac{2\beta_4 \sup_t(\|\bar{\boldsymbol{h}}_N(\boldsymbol{z}_{c,N}, \boldsymbol{z}_{c,M})\|)}{\beta_6} + \|\boldsymbol{z}^c_{orig,N}\|. \tag{46}$$

Proof: The proof is given in the appendix. □

The constants in Lemma 3 and Theorem 2 depend on the functions $\boldsymbol{f}_N(\cdot)$, $\boldsymbol{g}_N(\cdot)$, and $\boldsymbol{h}_N(\cdot)$ and thus on N. In addition, the observer dynamics (44) depend on the nonlinear filtering gain $\boldsymbol{K}_N(\cdot)$. In other words, proving that the solution to the approximate observer converges to the true state as the order of approximation increases requires adding some conditions on the upper bounds of these constants as well as some conditions necessary to show the convergence of the involved functions. Finding these conditions is not straightforward for general nonlinear PDEs.

According to Theorem 2, the estimation error bound depends on the model truncation defined by $\bar{\boldsymbol{h}}_N(\boldsymbol{z}_{c,N}, \boldsymbol{z}_{c,M})$ and $\mathbf{z}^c_{orig,N}$. If the norms of these terms converge to zero as the order of approximation increases, the estimation error norm converges to zero. This convergence is observed in the numerical simulation in the next section.

4. Simulations

In this section, the modified sliding mode observer is compared with different estimation methods for variations of the heat equation; linear, quasi-linear, and fully nonlinear versions are considered as well as versions with and without a disturbance input. In the following simulations, the EKF and the modified SMO are designed in the transformed coordinates defined by equations (4). The UKF is designed in the original coordinates. Two sources of uncertainties are introduced: the disturbance coming from the unknown input $\xi(t)$ and the modeling uncertainty due to the order reduction in the observer design.

The finite element method with piece-wise linear functions was used to approximate all three versions of the heat equation. The order of approximation is defined as the number of employed elements. The "true" system was simulated in COMSOL with seventeen linear elements to imitate true measurements and states. Increasing the number of elements beyond seventeen showed negligible changes in the system's solution.

In the continuous-time EKF, a differential Riccati equation must be solved simultaneously with the system's dynamical equations. It is faster to use the discrete-time version of the EKF. In order to use the discrete-time EKF, the time span of interest is divided into sub-intervals of the same size Δt where Δt is faster than the observer's dynamics so that the effect of time discretization can be neglected. The value $\Delta t = 0.01$ was found to be adequate.

The observer parameters were chosen by trial and error to achieve the best performance for each observer. This tuning was done separately for every observer. For example, the parameter a in the EKF algorithm (Table 1) provides control over the rate of convergence. The best value for a was found by increasing it to a point that the covariance matrix remained bounded and no further improvement of the performance was obtained. The same approach was used to find the SMO gain. In the standard SMO, which was added for the sake of comparison, the a Kalman filter was tuned using just the linear part of the system. In the modified SMO, the EKF was combined with the sliding mode observer. The UKF parameters were also chosen for the best performance too.

On every sub-interval, the observer's dynamical equations (44) were solved with $\boldsymbol{K}_N(t)$ set to zero. Next, the discrete-time EKF was used to provide the state estimate at every time step; the observer gain $\boldsymbol{K}_N(t)$ acts as a correction to the state prediction. The observer equations were solved using MATLAB ODE15s. Let the solution at the time step $k+1$ be

$$\boldsymbol{z}_{k+1} = \boldsymbol{\chi}(\Delta t, \boldsymbol{z}_k, u_{[t_k, t_{k+1}]}, \xi_{[t_k, t_{k+1}]}) \tag{47}$$

where $\boldsymbol{\chi}(\cdot)$ is an evolution operator. The connection between the linearization around the estimated state $\hat{\boldsymbol{z}}$ in the continuous-time and sampled-time system is provided by Theorem 3 in Appendix A. Theorem 3 was used to calculate the linearization of $\chi(\cdot)$ around the state estimate $\hat{\boldsymbol{z}}$ as the linear operator $\boldsymbol{F}_{\boldsymbol{z}_k}$ in Table 1.

Simulations were run first with a zero disturbance ξ and then with a non-zero ξ. In both sets, as a non-persistent source of disturbances, a fraction of the initial condition profile $\omega z(0, x)$ for $\omega > 0$ was added to the system's state at every time step. This type of disturbance was added to keep the system's modes excited in time. For linear and quasi-linear heat equations, $\omega = 0.1$, and for nonlinear equation, $\omega = 0.3$.

Letting z_M be the "true" state calculated with approximation order M, and $\hat{z}_N$ the estimated state using an approximation of order N, the estimation error is defined as

$$e_{est} = \sqrt{\int_{x=0}^{1} e^2 dx}$$

where $e = z_M - \hat{z}_N$. The system's initial condition is

$$z(0, x) = 0.5 \sin(\pi x) \operatorname{sech}(3(x - 0.5))$$

and the observer's initial condition is $\hat{z}(0, x) = 0$. The shared observer's parameters are chosen as, for the EKF,

$$\boldsymbol{P_\nu} = 0.1\boldsymbol{I}_{N\times N}, \quad \boldsymbol{P}_\omega = 0.1, \quad \boldsymbol{P}_{\boldsymbol{z}_0} = \boldsymbol{0}_{N\times N};$$

for the UKF,

$$\boldsymbol{P_\nu} = 0.1\boldsymbol{I}_{N\times N}, \quad \boldsymbol{P}_\omega = 0.1, \quad \alpha = 0.05, \quad \kappa = 0, \quad \beta = 2, \quad \boldsymbol{P}_{\boldsymbol{z}_0} = 10^{-6}\boldsymbol{I}_{N\times N};$$

and for the modified SMO,

$$\boldsymbol{P_\nu} = 0.1\boldsymbol{I}_{N\times N}, \quad \boldsymbol{P}_\omega = 0.1, \quad \boldsymbol{P}_{\boldsymbol{z}_0} = \boldsymbol{0}_{N\times N}.$$

The linear heat equation was

$$\frac{\partial z}{\partial t} = \frac{\partial}{\partial x}(\alpha_1 \frac{\partial z}{\partial x}) + b(x)u(t) + g(x)\xi(t) \tag{48}$$

$$\frac{\partial z}{\partial x}(0, t) = 0, \quad z(1, t) = 0, \tag{49}$$

and localized observation

$$y = \frac{1}{\delta} \int_{\frac{1}{2}-\delta}^{\frac{1}{2}+\delta} z(x)dx \tag{50}$$

where $\alpha_1 = 6$ is the diffusivity coefficient, $z \in \mathcal{L}_2(0, 1)$ is the state variable, $u(t)$ is the control input, $\xi(t)$ is an unknown input attributed to the disturbances, $g(x) \in \mathcal{C}([0, 1])$ is the spatial distribution of the unknown input, and $b(x) \in \mathcal{C}([0, 1])$ is the spatial distribution of the control. In the simulations,

$$g(x) = \sin(\pi x), \quad \xi(t) = 20 \sin(t), \quad b(x) = \sin(2\pi x), \quad u(t) = 10 \sin(t), \quad \delta = 10^{-4}.$$

The observer parameters are $a = 20, \quad \lambda_1 = 50$.

(Figures 1, 2, 3, and 4 near here)

The simulation results are shown in Figures 1, 2, and 3. These figures show that for all methods, the estimation error not surprisingly decreases by increasing the order of approximation. In the absence of an external disturbance input, both EKF and UKF show the same performance. Furthermore, the modified SMO performs closely to the EKF.

When the disturbance input is added, that is, $\xi \neq 0$, the EKF offers slightly better estimation error than the UKF. In the presence of the disturbance input, the modified SMO provides much smaller estimation error than the other estimation methods. The modified SMO shows a considerable decrease in error for higher orders of approximation. The error for different observation techniques with a fixed approximation order $N = 5$ is shown in Figure 4 and Table 3.

The next model considered was a reaction-diffusion system, the quasi-linear heat equation

$$\frac{\partial z}{\partial t} = \frac{\partial}{\partial x}(\alpha_2 \frac{\partial z}{\partial x}) + R(z) + b(x)u(t) + g(x)\xi(t) \tag{51}$$

where $\alpha_2 = 4$,

$$R(z) = \eta_1 z(\eta_2 - z),$$

$\eta_1 = 0.2$, and $\eta_2 = \pi^2$. The boundary conditions are again (49), and the observation is defined by equation (50). In the simulations,

$$g(x) = \sin(\pi x), \quad \xi(t) = -18(2 + 1.5\sin(t)), \quad b(x) = \sin(2\pi x), \quad u(t) = 10\sin(t).$$

The observer parameters are $a = 2, \lambda_1 = 40$ for the EKF and the modified SMO and $\lambda_1 = 60$ for the standard SMO.

(Figures 5, 6, 7, and 8 near here)

The simulation results are shown in Figures 5, 6, and 7. Again, the estimation error decreases as the order of approximation increases. Figures 5 and 6 indicate that in the absence of a disturbance input, the estimation error provided by both EKF and UKF is nearly the same. Moreover, adding the sliding term to the EKF does not change its performance when there is no disturbance.

However, the estimation error of the UKF in the existence of the disturbance input is more than two times larger than that of the EKF. According to Figure 7, the modified SMO reduces the estimation error four times more than EKF. This improvement can be seen in Figure 8 and Table 3 where different observation techniques, all with approximation order $N = 5$, are compared. It is also observed that the modified SMO produces an error that is almost a third of the one produced by the standard SMO.

The last model considered was a nonlinear heat equation. The system is similar to the linear equation (48) except that the diffusivity is a function of the state:

$$\alpha_3(z) = \theta_1(1 + \theta_2 z^2)$$

where $\theta_1 = 6$ and $\theta_2 = 0.02$. The governing equation is

$$\frac{\partial z}{\partial t} = \frac{\partial}{\partial x}(\alpha_3(z)\frac{\partial z}{\partial x}) + b(x)u(t) + g(x)\xi(t) \tag{52}$$

The same boundary conditions (49) hold, and the observation is again defined by (50). In the simulations,

$$g(x) = \sin(\pi x), \quad \xi(t) = 5.45(-2 + 1.5\sin(t)), \quad b(x) = \sin(2\pi x), \quad u(t) = 10\sin(t).$$

The observer parameters are $a = 20, \lambda_1 = 10$ for the EKF and the modified SMO and $\lambda_1 = 30$ for the standard SMO.

(Figures 9, 10, 11, and 12 near here)

The simulation results are shown in Figures 9, 10, and 11. The same pattern of reduction in error as the order of approximation increases can be seen in the absence of a disturbance input. The estimation error of both EKF and UKF are almost the same in the absence of the disturbance (Figures 9 and 10). However, the estimation error associated with the UKF is larger than that of the EKF when the disturbance is present. Like the previous two examples of the heat equations, the modified SMO performs similarly to the EKF when there is no disturbance. However, when the disturbance is present, with the modified SMO, the error is up to four times smaller than the EKF (Figure 11). This is illustrated in Figure 12 and Table 3 where all the observation methods are compared with the order of approximation $N = 5$. It is also observed that the modified SMO produces an error around four time smaller than the error produced by standard SMO.

5. Conclusions

The main contribution of this paper was a modified SMO where an EKF was combined with a SMO. This modified SMO combines an exponential stabilizing nonlinear observer with the sliding mode observation to increase the estimation performance. Unlike standard versions of the SMO, the modified version handles both nonlinearities and disturbances. The exponential convergence of the estimation error to zero was proven in Theorem 1. The modified SMO was compared with two nonlinear filtering methods, the EKF and UKF, as well as a standard SMO for estimation of three different versions of heat equation: linear, quasi-linear, and nonlinear. The simulations were run for each model and estimator with and without an external disturbance.

Although chattering is less of an issue in a sliding mode observer than in a sliding mode control, and was not an issue in our computations, discontinuities in the observer dynamics may cause complications. Specifically, large discontinuities may lead to an increase in computation time to solve the observer equations. However, the modified SMO provides the possibility of using smaller sliding gains, which reduce chattering. Table 3 shows that the computation time of the modified SMO did not increase significantly compared with the EKF and UKF.

In the simulations, the order of approximation used to design the observer was smaller than the order used for the "true" system to simulate the effect of neglected modes. Therefore, the error was expected to be only bounded as given by Theorem 2. In the absence of the external disturbance, increasing the order of approximation decreases the error, which is not surprising. Increasing the order of approximation results in a closer approximation to the true system.

When the disturbance was present, the performance of the modified SMO was better than that of the other observers, including EKF and standard SMO. Exponential convergence to zero of the error norm, proved in Theorem 1, can be observed for high orders of approximation in Figures 3, 7, and 11. Furthermore, increasing the order of approximation reduces the estimation error, as prediced by Theorem 2. According to this theorem, the estimation error bound is defined by the norm of model truncation denoted by $\bar{\boldsymbol{h}}_N(\boldsymbol{z}_{c,N}, \boldsymbol{z}_{c,M})$ and $\mathbf{z}^c_{orig,N}$; the decreasing estimation error norm observed in the simulations is assigned with the convergence of these terms to zero as the order of approximation increases.

The performance of the modified SMO was examined with different versions of the heat equation. The heat equation is structurally stable and satisfies the conditions of the Theorem 1 and 2; however, the wave equation has different dynamics and stability properties which limit the application of the SMO. Future work involves development of observers for DPSs such as weakly damped waves where the decline in energy with each mode is much slower than for diffusion equations.

Acknowledgement

The authors would like to acknowledge the financial support of the Ontario Research Fund and Automotive Partnership Canada in this work.

References

Castillo, F., Witrant, E., Prieur, C., Dugard, L., 2013. Boundary observers for linear and quasi-linear hyperbolic systems with application to flow control. Automatica 49 (11), 3180–3188.

Chen, F., Dunnigan, M., 2002. Comparative study of a sliding-mode observer and Kalman filters for full state estimation in an induction machine. IEE Proceedings-Electric Power Applications 149 (1), 53–64.

Curtain, R. F., 1982. Finite-dimensional compensator design for parabolic distributed systems with point sensors and boundary input. IEEE Transactions on Automatic Control 27 (1), 98–104.

Curtain, R. F., Zwart, H., 1995. An introduction to infinite-dimensional linear systems theory. Springer New York.

Demetriou, M. A., 2004. Natural second-order observers for second-order distributed parameter systems. Systems & control letters 51 (3), 225–234.

Ding, X., Frank, P. M., Guo, L., 1990. Nonlinear observer design via an extended observer canonical form. Systems & control letters 15 (4), 313–322.

Drakunov, S., Utkin, V., 1995. Sliding mode observers. tutorial. In: Proceedings of the 34th IEEE Conference on Decision and Control. Vol. 4. IEEE, pp. 3376–3378.

Drakunov, S. V., 1992. Sliding-mode observers based on equivalent control method. In: Proceedings of the 31st IEEE Conference on Decision and Control. IEEE, pp. 2368–2369.

Drakunov, S. V., Reyhanoglu, M., 2011. Hierarchical sliding mode observers for distributed parameter systems. Journal of Vibration and Control 17 (10), 1441–1453.

Edwards, C., Spurgeon, S., 1998. Sliding mode montrol: theory and applications. CRC Press.

Einicke, G. A., White, L. B., 1999. Robust extended Kalman filtering. IEEE Transactions on Signal Processing 47 (9), 2596–2599.

Fridman, L., Shtessel, Y., Edwards, C., Yan, X. G., 2008. Higher-order sliding-mode observer for state estimation and input reconstruction in nonlinear systems. International Journal of Robust and Nonlinear Control 18 (4-5), 399–412.

Grewal, M. S., Andrews, A. P., 2011. Kalman filtering: theory and practice using MATLAB. John Wiley & Sons.

Hidayat, Z., Babuska, R., De Schutter, B., Nunez, A., 2011. Observers for linear distributed-parameter systems: A survey. In: Robotic and Sensors Environments (ROSE), 2011 IEEE International Symposium on. IEEE, pp. 166–171.

Isidori, A., 1995. Nonlinear control systems. Vol. 1. Springer.

Kai, X., Liangdong, L., Yiwu, L., 2011. Robust extended Kalman filtering for nonlinear systems with multiplicative noises. Optimal Control Applications and Methods 32 (1), 47–63.

Kai, X., Wei, C., Liu, L., 2010. Robust extended Kalman filtering for nonlinear systems with stochastic uncertainties. Systems, Man and Cybernetics, Part A: Systems and Humans, IEEE Transactions on 40 (2), 399–405.

Kazantzis, N., Kravaris, C., 1998. Nonlinear observer design using Lyapunov's auxiliary theorem. Systems & Control Letters 34 (5), 241–247.

Koshkouei, A. J., Zinober, A. S., 2004. Sliding mode state observation for non-linear systems. International Journal of Control 77 (2), 118–127.

Liu, Y. A., Lapldus, L., 1976. Observer theory for distributed-parameter systems. International Journal of Systems Science 7 (7), 731–742.

Meirovitch, L., Baruh, H., 1983. On the problem of observation spillover in self-adjoint distributed-parameter systems. Journal of Optimization Theory and Applications 39 (2), 269–291.

Miranda, R., Chairez, I., Moreno, J., 2010. Observer design for a class of parabolic PDE via sliding modes and backstepping. In: 2010 11th International Workshop on Variable Structure Systems (VSS). IEEE, pp. 215–220.

Misawa, E., Hedrick, J., 1989. Nonlinear observers—a state-of-the-art survey. Journal of dynamic systems, measurement, and control 111 (3), 344–352.

Noh, D., Jo, N. H., Seo, J. H., 2004. Nonlinear observer design by dynamic observer error linearization. Automatic Control, IEEE Transactions on 49 (10), 1746–1753.

Orlov, Y. V., 2008. Discontinuous systems: Lyapunov analysis and robust synthesis under uncertainty conditions. Springer Science & Business Media.

Reif, K., Sonnemann, F., Unbehauen, R., 1998. An EKF-based nonlinear observer with a prescribed degree

of stability. Automatica 34 (9), 1119–1123.
Reif, K., Sonnemann, F., Unbehauen, R., 1999. Nonlinear state observation using h/sub/spl infin//-filtering riccati design. Automatic Control, IEEE Transactions on 44 (1), 203–208.
Reif, K., Unbehauen, R., 1999. The extended Kalman filter as an exponential observer for nonlinear systems. IEEE Transactions on Signal Processing 47 (8), 2324–2328.
Rigatos, G. G., 2011. Derivative-free nonlinear Kalman filtering for MIMO dynamical systems: application to multi-DOF robotic manipulators. International Journal of Advanced Robotic Systems 8 (6), 47–61.
Rigatos, G. G., 2015a. Control of heat diffusion in arc welding using differential flatness theory and nonlinear Kalman filtering. IFAC-PapersOnLine 48 (3), 1368–1374.
Rigatos, G. G., 2015b. Nonlinear control and filtering using differential flatness approaches: applications to electromechanical systems. Vol. 25. Springer.
Sallberg, S. A., Maybeck, P. S., Oxley, M. E., 2010. Infinite-dimensional sampled-data Kalman filtering and the stochastic heat equation. In: Decision and Control (CDC), 2010 49th IEEE Conference on. IEEE, pp. 5062–5067.
Smyshlyaev, A., Krstic, M., 2005. Backstepping observers for a class of parabolic PDE's. Systems & Control Letters 54 (7), 613–625.
Spurgeon, S. K., 2008. Sliding mode observers: a survey. International Journal of Systems Science 39 (8), 751–764.
Utkin, V., 1999. Sliding mode estimation and optimization methods in nonlinear control problems. Ph.D. thesis, The Ohio State University.
Veluvolu, K., Soh, Y., Cao, W., 2007a. Robust observer with sliding mode estimation for nonlinear uncertain systems. Control Theory & Applications, IET 1 (5), 1533–1540.
Veluvolu, K., Soh, Y., Cao, W., 2007b. Robust observer with sliding mode estimation for nonlinear uncertain systems. Control Theory & Applications, IET 1 (5), 1533–1540.
Walcott, B., Corless, M., Żak, S., 1987. Comparative study of non-linear state-observation techniques. International Journal of Control 45 (6), 2109–2132.
Walcott, B., Zak, S., 1987. State observation of nonlinear uncertain dynamical systems. IEEE Transactions on Automatic Control 32 (2), 166–170.
Wan, E. A., Van Der Merwe, R., 2000. The unscented Kalman filter for nonlinear estimation. In: Adaptive Systems for Signal Processing, Communications, and Control Symposium 2000. AS-SPCC. IEEE, pp. 153–158.
Wu, H.-N., Li, H.-X., 2008. H_∞ fuzzy observer-based control for a class of nonlinear distributed parameter systems with control constraints. IEEE Transactions on Fuzzy Systems 16 (2), 502–516.
Wu, H. N., Li, H. X., 2011. Robust adaptive neural observer design for a class of nonlinear parabolic PDE systems. Journal of Process Control 21 (8), 1172–1182.
Xia, X. H., Gao, W. B., 1989. Nonlinear observer design by observer error linearization. SIAM Journal on Control and Optimization 27 (1), 199–216.
Xiong, Y., Saif, M., 2001. Sliding mode observer for nonlinear uncertain systems. IEEE Transactions on Automatic Control 46 (12), 2012–2017.

Appendix A. Appendix

Proof of Lemma 3:

Consider a continuously differentiable Lyapunov function $V(\cdot)$ similar to what is chosen in Lemma 2 satisfying Assumption 5. Followed by the same procedure as in Lemma 2, along the trajectories given by (45),

$$\frac{dV(\boldsymbol{e}_N)}{dt} \leq -\beta_3\|\boldsymbol{e}_N\|^2 + \beta_4\|\boldsymbol{\Gamma}_N(\boldsymbol{z}_{c,N})\xi - \boldsymbol{u}_{r,N} + \bar{\boldsymbol{h}}_N(\boldsymbol{z}_{c,N}, \boldsymbol{z}_{c,M})\|\|\boldsymbol{e}_N\|. \tag{A1}$$

From the definition of $\boldsymbol{\Gamma}_N(\boldsymbol{z}_{c,N})$; equation (7); Lemma 1; Assumption 4; and the boundedness of the vector $\boldsymbol{u}_{r,N}$, unknown input ξ, and $\bar{\boldsymbol{h}}_N(\boldsymbol{z}_{c,N}, \boldsymbol{z}_{c,M})$, it can be concluded that for some $M_d > 0$,

$$\|\boldsymbol{\Gamma}_N(\boldsymbol{z}_{c,N})\xi - \boldsymbol{u}_{r,N} + \bar{\boldsymbol{h}}_N(\boldsymbol{z}_{c,N}, \boldsymbol{z}_{c,M})\| \leq M_d + M_h.$$

Therefore,

$$\frac{dV(\boldsymbol{e}_N)}{dt} \leq -\beta_3\|\boldsymbol{e}_N\|^2 + \beta_4(M_d + M_h)\|\boldsymbol{e}_N\|,$$

and

$$\|\boldsymbol{e}_N\| \leq \frac{\beta_4(M_d + M_h)}{\beta_3}.$$

Since the error vector and the system state are bounded so is the observer state, and the proof is complete. □

Proof of Theorem 2:
If the disturbance input ξ is zero, the result follows trivially from the assumptions. Consider then a non-zero disturbance term $\xi \neq 0$. The proof is similar to that of Theorem 1. Followed by the same procedure as in the step one of the proof of this theorem, for $q = 1$, there exists $\lambda_1 > 0$ such that the observer reaches the sliding surface in finite time; the equivalent signal is

$$\boldsymbol{u}_{eq,N} = \begin{bmatrix} \bar{\boldsymbol{C}}_N(\bar{\boldsymbol{f}}_N(\boldsymbol{z}_{c,N}) - \bar{\boldsymbol{f}}_N(\hat{\boldsymbol{z}}_{c,N})) + \\ \bar{\boldsymbol{C}}_N(\bar{\boldsymbol{g}}_N(\boldsymbol{z}_{c,N}, u(t)) - \bar{\boldsymbol{g}}_N(\hat{\boldsymbol{z}}_{c,N}, u(t))) + \\ \bar{\boldsymbol{C}}_N\boldsymbol{\Gamma}_N(\boldsymbol{z}_{c,N})\xi(t) + \\ \bar{\boldsymbol{C}}_N\bar{\boldsymbol{h}}_N(\boldsymbol{z}_{c,N}, \boldsymbol{z}_{c,N}) \\ \boldsymbol{0}_{(n-1)\times 1} \end{bmatrix}, \tag{A2}$$

where $\bar{\boldsymbol{C}}_N = [1, 0, \ldots, 0]$ is a row matrix of dimension N. From equation (A2) and the inequalities (8),

$$\|\boldsymbol{\Gamma}_N(\boldsymbol{z}_{c,N})\xi - \boldsymbol{u}_{eq,N}\| \leq (1 + M_a + M_q)\|\boldsymbol{e}\| + \|\bar{\boldsymbol{h}}_N(\boldsymbol{z}_{c,N}, \boldsymbol{z}_{c,M})\|. \tag{A3}$$

In sliding mode, which occurs after a finite time, differentiating the Lyapunov function $V(\cdot)$, which satisfies Assumption 5 leads to

$$\frac{dV(\boldsymbol{e}_N)}{dt} = V_0(\boldsymbol{e}_N) + \frac{\partial V(\boldsymbol{e}_N)}{\partial \boldsymbol{e}_N}(\boldsymbol{\Gamma}_N(\boldsymbol{z}_{c,N})\xi - \boldsymbol{u}_{eq,N} + \bar{\boldsymbol{h}}_N(\boldsymbol{z}_{c,N}, \boldsymbol{z}_{c,M})). \tag{A4}$$

Inequalities (15), (14) and (A3) imply that

$$\frac{dV(\boldsymbol{e}_N)}{dt} \leq -\beta_3\|\boldsymbol{e}_N\|^2 + \beta_4(1 + M_a + M_q)\|\boldsymbol{e}_N\|^2 + 2\beta_4 \sup_t(\|\bar{\boldsymbol{h}}_N(\boldsymbol{z}_{c,N}, \boldsymbol{z}_{c,M})\|)\|\boldsymbol{e}_N\|. \tag{A5}$$

Since $\beta_3 > \beta_4(1 + M_a + M_q)$, for some $\beta_6 = \beta_3 - \beta_4(1 + M_a + M_q) > 0$

$$\frac{dV(\boldsymbol{e}_N)}{dt} \leq -\beta_6\|\boldsymbol{e}_N\|^2 + 2\beta_4 \sup_t(\|\bar{\boldsymbol{h}}_N(\boldsymbol{z}_{c,N}, \boldsymbol{z}_{c,M})\|)\|\boldsymbol{e}_N\| \tag{A6}$$

and the estimation error $\boldsymbol{e}$ is bounded by (46).

□

Theorem 3: *Assume that the nonlinear function $\boldsymbol{f}(\cdot)$ given in equation (1) is second-order differentiable, and (1) has a solution on $[t_k, t_{k+1}]$ in an evolution form (47) in which $\boldsymbol{\chi}(\cdot)$ is also second-order differentiable with respect to the vector $\boldsymbol{z}_k$. Let the linearization of $\boldsymbol{f}(\cdot)$ be defined by*

$$\boldsymbol{A}_{\bar{\boldsymbol{z}}} = \frac{\partial \boldsymbol{f}(\boldsymbol{z})}{\partial \boldsymbol{z}} \mid_{\bar{\boldsymbol{z}}}$$

for some $\bar{\boldsymbol{z}} \in \mathbb{R}^n$. Furthermore, let the linearization of the evolution operator be defined as

$$\boldsymbol{F}_{\bar{\boldsymbol{z}}}(\Delta t, u_{[t_k,t_{k+1}]}) = \frac{\partial \boldsymbol{\chi}(\Delta t, \boldsymbol{z}_k, u_{[t_k,t_{k+1}]}, \xi_{[t_k,t_{k+1}]})}{\partial \boldsymbol{z}} \mid_{(\Delta t, \bar{\boldsymbol{z}}, u_{[t_k,t_{k+1}]}, 0)} .$$

Then, the operator $\boldsymbol{F}_{\bar{\boldsymbol{z}}_k}(\cdot)$ is the evolution operator generated by the linear operator $\boldsymbol{A}_{\bar{\boldsymbol{z}}}$ when the disturbance term is set to zero. In addition,

$$\frac{\partial \boldsymbol{F}_{\bar{\boldsymbol{z}}}(\Delta t, u_{[t_k,t_{k+1}]})}{\partial u_{[t_k,t_{k+1}]}} = 0.$$

Proof: Let $\boldsymbol{z}(t)$ be a solution to the system dynamical equation (1); the time differentiation of this signal at time t can be defined as

$$\frac{d\boldsymbol{z}(t)}{dt} = \lim_{\Delta t \to 0} \frac{\boldsymbol{z}(t+\Delta t) - \boldsymbol{z}(t)}{\Delta t}. \tag{A7}$$

Now, by substituting equation (47) and (1) into (A7) and setting $\xi(t) = 0$, it is obtained that

$$\boldsymbol{f}(\boldsymbol{z}(t)) + \boldsymbol{B}u = \lim_{\Delta t \to 0} \frac{\boldsymbol{\chi}(\Delta t, \boldsymbol{z}(t), u_{[t,t+\Delta t]}, 0) - \mathbf{z}(\mathbf{t})}{\Delta t}. \tag{A8}$$

The expansion of the nonlinear function $\boldsymbol{f}(\boldsymbol{z})$ around the arbitrary vector $\bar{\boldsymbol{z}}$ reads as

$$\begin{aligned} \boldsymbol{f}(\boldsymbol{z}(t)) =& \boldsymbol{f}(\bar{\boldsymbol{z}}(t)) + \boldsymbol{A}_{\bar{\boldsymbol{z}}}(\boldsymbol{z}(t) - \bar{\boldsymbol{z}}(t)) + \\ & \sum_{i,j} \frac{\partial}{\partial z_i} \frac{\partial \boldsymbol{f}}{\partial z_j} \mid_{\check{\boldsymbol{z}}_1} (z_i(t) - \bar{z}_i(t))(z_j(t) - \bar{z}_j(t)) \end{aligned} \tag{A9}$$

$\check{\boldsymbol{z}}_1(t) \in [\bar{\boldsymbol{z}}(t), \boldsymbol{z}(t)]$ for every t. Similarly, the evolution operator can also be expanded around the arbitrary vector $\bar{z}$ as

$$\begin{aligned} & \boldsymbol{\chi}(\Delta t, \boldsymbol{z}(t), u_{[t,t+\Delta t]}, 0) = \\ & \quad \boldsymbol{\chi}(\Delta t, \bar{\boldsymbol{z}}(t), u_{[t,t+\Delta t]}, 0) + \\ & \quad \boldsymbol{F}_{\bar{\boldsymbol{z}}(t)}(\Delta t, u_{[t,t+\Delta t]})(\boldsymbol{z}(t) - \bar{\boldsymbol{z}}(t)) + \\ & \quad \sum_{i,j} \frac{\partial}{\partial z_i} \frac{\partial \boldsymbol{\chi}}{\partial z_j} \mid_{(\Delta t, \check{\boldsymbol{z}}_2, u_{[t,t+\Delta t]}, 0)} (z_i(t) - \bar{z}_i(t))(z_j(t) - \bar{z}_j(t)) \end{aligned} \tag{A10}$$

where $\check{\boldsymbol{z}}_2(t) \in [\bar{\boldsymbol{z}}(t), \boldsymbol{z}(t)]$ for every t.

Substituting equations (A9) and (A10) into (A8) and employing equation (A8) for $\boldsymbol{z} = \bar{\boldsymbol{z}}$ result in

$$\begin{aligned}
&\boldsymbol{A}_{\bar{\boldsymbol{z}}}(\boldsymbol{z}(t)-\bar{\boldsymbol{z}}(t))+\\
&\sum_{i,j}\frac{\partial}{\partial z_i}\frac{\partial \boldsymbol{f}}{\partial z_j}\mid_{\check{\boldsymbol{z}}_1}(z_i(t)-\bar{z}_i(t))(z_j(t)-\bar{z}_j(t))=\\
&\lim_{\Delta t\to 0}\frac{\boldsymbol{F}_{\bar{\boldsymbol{z}}(t)}(\Delta t,u_{[t,t+\Delta t]})(\boldsymbol{z}(t)-\bar{\boldsymbol{z}}(t))-(\boldsymbol{z}(t)-\bar{\boldsymbol{z}}(t))}{\Delta t}+\\
&\lim_{\Delta t\to 0}\frac{\sum_{i,j}\frac{\partial}{\partial z_i}\frac{\partial \boldsymbol{\chi}}{\partial z_j}\mid_{(\Delta t,\check{\boldsymbol{z}}_2,u_{[t,t+\Delta t]},0)}(z_i(t)-\bar{z}_i(t))(z_j(t)-\bar{z}_j(t))}{\Delta t}.
\end{aligned} \tag{A11}$$

Since equation (A11) is satisfied for all $\boldsymbol{z},\bar{\boldsymbol{z}}\in C^1([0,T],\mathbb{R}^n)$, it can be concluded that

$$\begin{aligned}
&\boldsymbol{A}_{\bar{\boldsymbol{z}}}(\boldsymbol{z}(t)-\bar{\boldsymbol{z}}(t))=\\
&\quad\lim_{\Delta t\to 0}\frac{\boldsymbol{F}_{\bar{\boldsymbol{z}}(t)}(\Delta t,u_{[t,t+\Delta t]})(\boldsymbol{z}(t)-\bar{\boldsymbol{z}}(t))-(\boldsymbol{z}(t)-\bar{\boldsymbol{z}}(t))}{\Delta t}
\end{aligned}$$

which simply indicates that $\boldsymbol{A}_{\bar{\boldsymbol{z}}}(\boldsymbol{z}(t)-\bar{\boldsymbol{z}}(t))$ generates $\boldsymbol{F}_{\bar{\boldsymbol{z}}(t)}(\Delta t,u_{[t,t+\Delta t]})(\boldsymbol{z}(t)-\bar{\boldsymbol{z}}(t))$ and is independent of the input vector $u(t)$. □

Table 1. Extended Kalman filtering algorithm

Initialize at $k = 0$:
$\hat{\boldsymbol{z}}_0 = E[\boldsymbol{z}_0]$,
$\boldsymbol{P}_{\boldsymbol{z}_0} = E[(\boldsymbol{z}_0 - \hat{\boldsymbol{z}}_0)(\boldsymbol{z}_0 - \hat{\boldsymbol{z}}_0)^T]$,
$\boldsymbol{P}_{\boldsymbol{\nu}} = E[(\boldsymbol{\nu} - \bar{\boldsymbol{\nu}})(\boldsymbol{\nu} - \bar{\boldsymbol{\nu}})^T]$,
$\boldsymbol{P}_{\omega} = E[(\omega - \bar{\omega})(\omega - \bar{\omega})^T]$.
For $k = 1, 2, \cdots, \infty$,
Prediction step:
Calculate the state variables prediction $\hat{\boldsymbol{c}}_N^-(t_{k+1})$, $\hat{\boldsymbol{\varphi}}_M^-(t_{k+1})$, and $\hat{\boldsymbol{\theta}}^-(t_{k+1})$ from (??)-(??).
Calculate the covarience matrix prediction $\boldsymbol{P}_N^-(t_{k+1})$ from (??).
Correction step:
Calculated the filtering gain from (??).
Update the state variables estimate $\hat{\boldsymbol{c}}_N(t_{k+1})$, $\hat{\boldsymbol{\varphi}}_M(t_{k+1})$, and $\hat{\boldsymbol{\theta}}(t_{k+1})$

Table 2. Unscented Kalman filtering

Initialize at $k = 0$:
$\hat{\boldsymbol{z}}_0 = E[\boldsymbol{z}_0]$,
$\boldsymbol{P}_{\boldsymbol{z}_0} = E[(\boldsymbol{z}_0 - \hat{\boldsymbol{z}}_0)(\boldsymbol{z}_0 - \hat{\boldsymbol{z}}_0)^T]$.
$\boldsymbol{P}_{\boldsymbol{\nu}} = E[(\boldsymbol{\nu} - \bar{\boldsymbol{\nu}})(\boldsymbol{\nu} - \bar{\boldsymbol{\nu}})^T]$,
$\boldsymbol{P}_{\omega} = E[(\omega - \bar{\omega})(\omega - \bar{\omega})^T]$.
For $k = 1, \cdots, \infty$,
Calculate Sigma points via equation (3), $\boldsymbol{z}_{s,i}$
Prediction step:
$\boldsymbol{z}_{s,i}^- = \boldsymbol{f}_d(\boldsymbol{z}_{s,i}) + \boldsymbol{B}_d u$, $i = 0, \ldots 2N$,
$\hat{\boldsymbol{z}}_k^- = \sum_{i=0}^{2N} W_i^m(\boldsymbol{Z}_{s,i})$,
$\boldsymbol{P}_{\boldsymbol{z}_k}^- = \sum_{i=0}^{2N} W_i^c((\boldsymbol{z}_{s,i}) - \hat{\boldsymbol{z}}_k^-)((\boldsymbol{z}_{s,i}) - \hat{\boldsymbol{z}}_k^-)^T + \boldsymbol{P}_{\boldsymbol{\nu}}$,
$y_{s,i} = h(\boldsymbol{z}_{s,i})$, $i = 0, \ldots 2N$
$\hat{y}_k^- = \sum_{i=0}^{2N} W_i^m(y_{s,i})$.
Correction step:
$\boldsymbol{P}_{y_k} = \sum_{i=0}^{2N} W_i^c(y_{s,i} - \hat{y}_k^-)(y_{s,i} - \hat{y}_k^-)^T + \boldsymbol{P}_{\omega}$,
$\boldsymbol{P}_{\boldsymbol{z}_k y_k} = \sum_{i=0}^{2N}(\boldsymbol{z}_{s,i} - \hat{\boldsymbol{z}}_k^-)(y_{s,i} - \hat{y}_k^-)^T$,
$\boldsymbol{K}_k = \boldsymbol{P}_{\boldsymbol{z}_k y_k}\boldsymbol{P}_{y_k}^{-1}$,
$\hat{\boldsymbol{z}}_k = \hat{\boldsymbol{z}}_k^- + \boldsymbol{K}_k(y_k - \hat{y}_k^-)$,
$\boldsymbol{P}_{\boldsymbol{z}_k} = \boldsymbol{P}_{\boldsymbol{z}_k}^- - \boldsymbol{K}_k\boldsymbol{P}_{y_k}\boldsymbol{K}_k^T$.

Table 3. Estimation error for different observation methods after transient period.

		Undisturbed		Disturbed	
	Method	Computation time	Error max	Computation time	Error max
Linear heat	EKF	77.6289	0.0022	135.4456	0.3227
	UKF	114.9613	0.0075	184.2440	0.3975
	SMO	82.0645	0.0053	193.6996	0.0480
Quasi-linear heat	EKF	200.6813	0.0053	207.3505	0.0886
	UKF	246.0649	0.0086	255.1652	0.3562
	SMO-EKF	102.7612	0.0060	117.8632	0.0190
	SMO	69.4914	0.0090	73.3460	0.0491
Nonlinear heat	EKF	168.2633	0.0019	177.9907	0.0566
	UKF	209.0683	0.0060	215.6899	0.1797
	SMO-EKF	178.3828	0.0036	186.0943	0.0138
	SMO	167.7243	0.0053	177.4914	0.0532

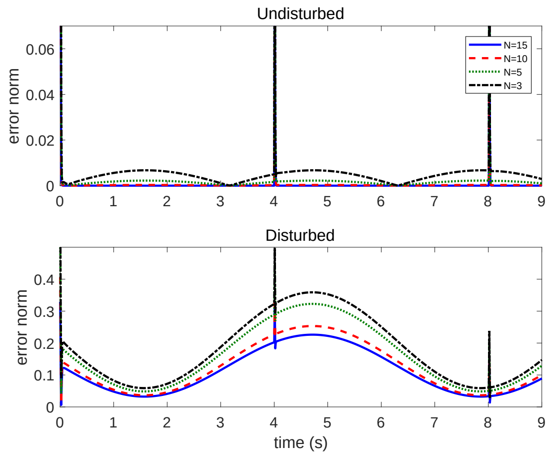

Figure 1. Estimation error of the EKF against time applied to the linear heat equation with different orders of approximation N. In the absence of a disturbance input, the error is very small even for $N = 5$. When the disturbance is present, the error is significant.

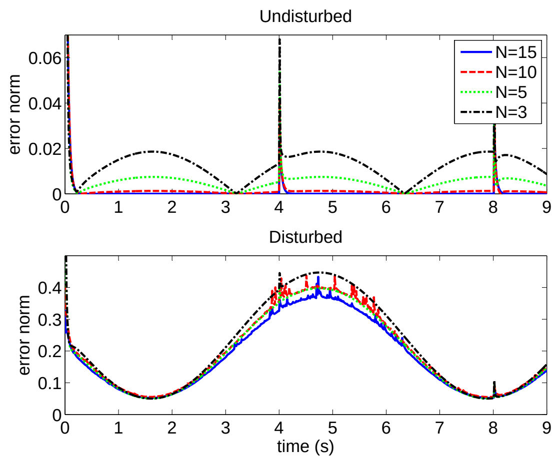

Figure 2. Estimation error of the UKF against time applied to the linear heat equation with different orders of approximation N. In the absence of a disturbance input, the error is very small even for $N = 5$. When the disturbance is present, the error is significant.

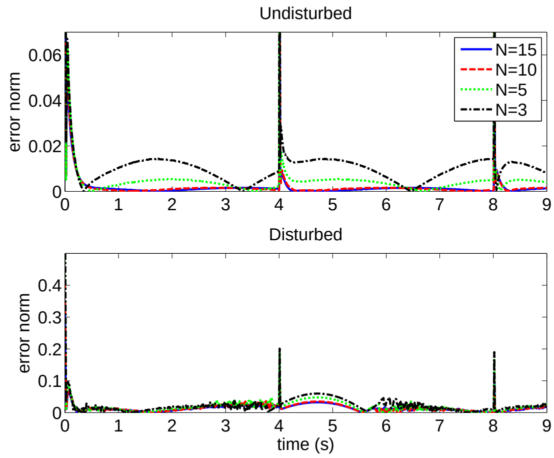

Figure 3. Estimation error of the modified SMO against time applied to the linear heat equation with different orders of approximation N. In the absence of a disturbance input, the error is very small even for $N = 5$. When the disturbance is present, the error is still small.

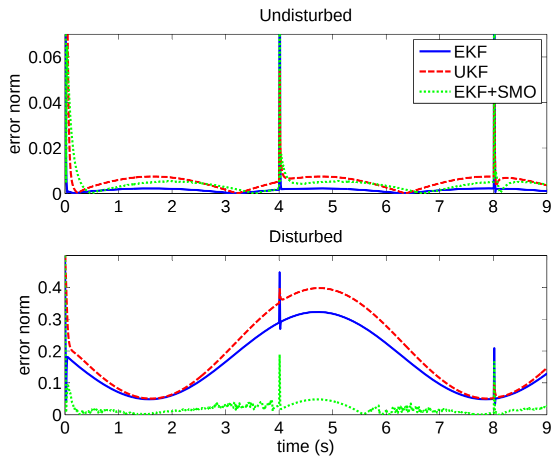

Figure 4. Comparison of different estimation methods, the EKF, UKF, and modified SMO, in estimating the state vector of the linear heat equation for the order of approximation $N = 5$.

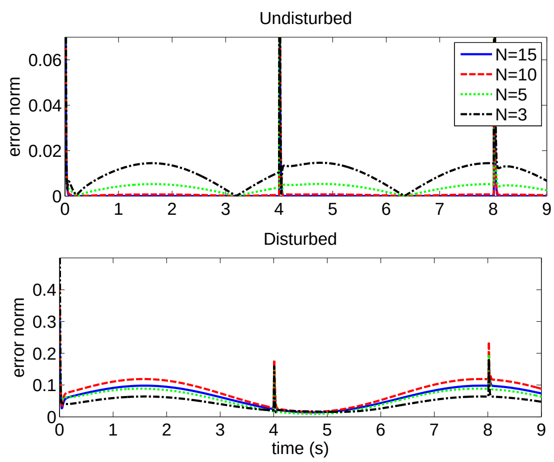

Figure 5. Estimation error of the EKF against time applied to the quasi-linear heat equation with different orders of approximation N. In the absence of a disturbance input, the error is very small even for $N = 5$. When the disturbance is present, the error increases.

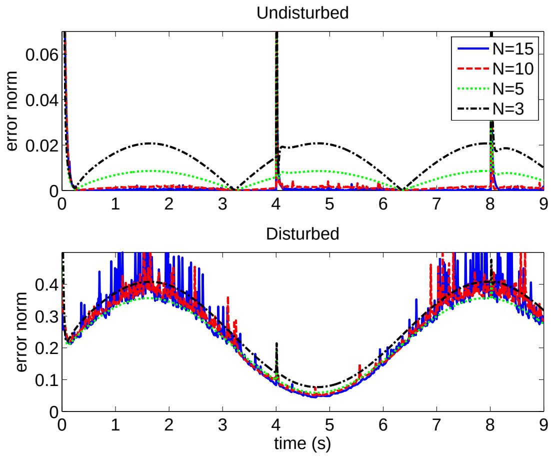

Figure 6. Estimation error of the UKF against time applied to the quasi-linear heat equation with different orders of approximation N. In the absence of a disturbance input, the error is very small even for $N = 5$. When the disturbance is present, the error is significant.

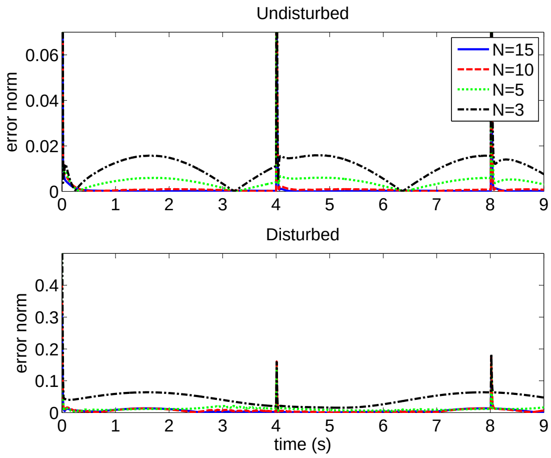

Figure 7. Estimation error of the modified SMO against time applied to the quasi-linear heat equation with different orders of approximation N. In the absence of a disturbance input, the error is very small even for $N = 5$. When the disturbance is present, the error is still small.

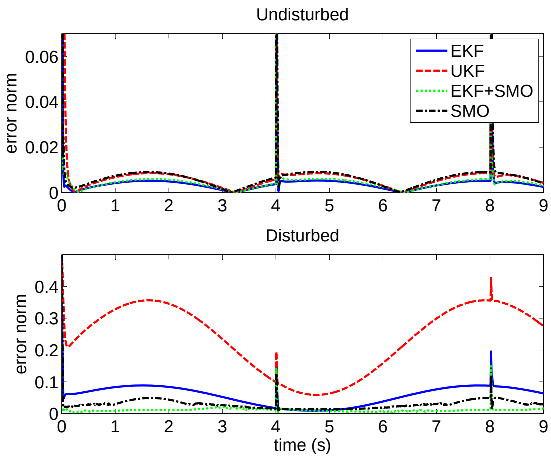

Figure 8. Comparison of different estimation methods, the EKF, UKF, and modified SMO in estimating the state vector of the quasi-linear heat equation for the order of approximation $N = 5$.

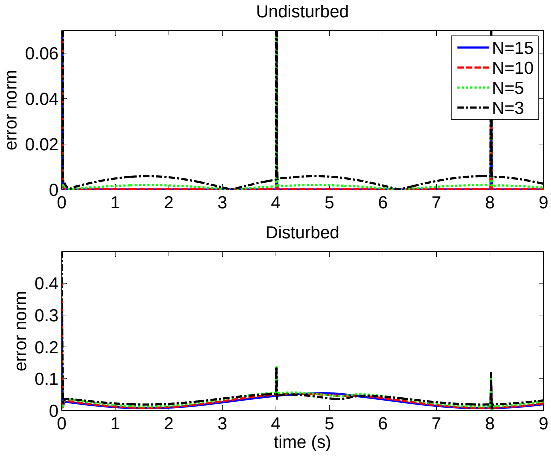

Figure 9. Estimation error of the EKF against time applied to the nonlinear heat equation with different orders of approximation N. In the absence of a disturbance input, the error is very small even for $N = 5$. When the disturbance is present, the error increases.

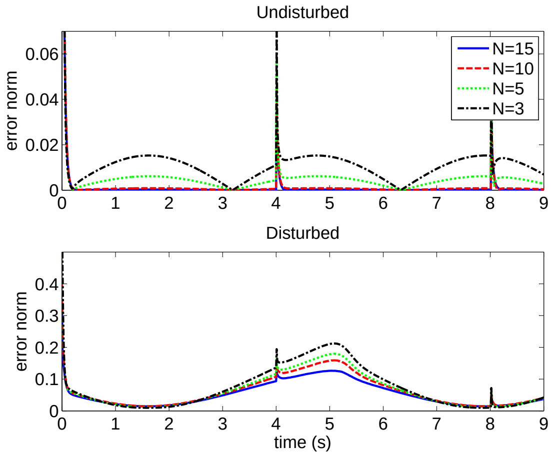

Figure 10. Estimation error of the UKF against time applied to the nonlinear heat equation with different orders of approximation N. In the absence of a disturbance input, the error is very small even for $N = 5$. When the disturbance is present, the error is significant.

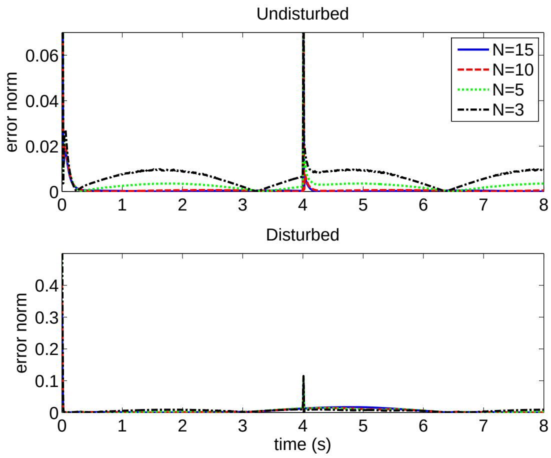

Figure 11. Estimation error of the modified SMO against time applied to the nonlinear heat equation with different orders of approximation N. In the absence of a disturbance input, the error is very small even for $N = 5$. When the disturbance is present, the error is still small.

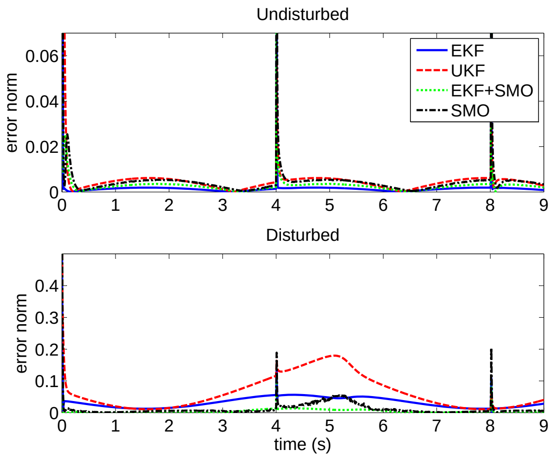

Figure 12. Comparison of different estimation methods, the EKF, UKF, and modified SMO in estimating the state vector of the nonlinear heat equation for the order of approximation $N = 5$.